AMERICAN UNIVERSITY OF BEIRUT

TRAJECTORY TRACKING OF AUTONOMOUS VEHICLES VIA MODEL PREDICTIVE CONTROL AIDED BY SLIDING MODE CONTROL

by
HASSAN ISSA EL ATWI

A thesis
submitted in partial fulfillment of the requirements
for the degree of Master of Engineering
to the Department of Electrical and Computer Engineering
of the Maroun Semaan Faculty of Engineering and Architecture
at the American University of Beirut

Beirut, Lebanon
January 2021
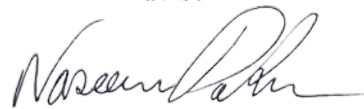
AMERICAN UNIVERSITY OF BEIRUT

TRAJECTORY TRACKING OF AUTONOMOUS VEHICLES VIA MODEL PREDICTIVE CONTROL AIDED BY SLIDING MODE CONTROL

by
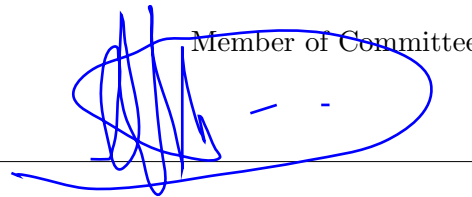HASSAN ISSA EL ATWI

Approved by:

_____

Dr. Naseem Daher, Assistant Professor   Advisor

Electrical and Computer Engineering

_____

Dr. Imad Elhajj ,Professor   Member of Committee

Electrical and Computer Engineering

_____

Dr. Elie Shammas, Associate Professor   Member of Committee

Mechanical Engineering

Date of thesis defense: January 26, 2021

AMERICAN UNIVERSITY OF BEIRUT

THESIS, DISSERTATION, PROJECT RELEASE FORM
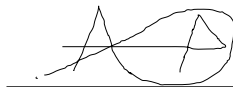
Student Name: __El Atwi_____Hassan_____Issa____
                        Last   First   Middle

☑ Master's Thesis   ◯ Master's Project   ◯ Doctoral Dissertation

☐   I authorize the American University of Beirut to: (a) reproduce hard or electronic copies of my thesis, dissertation, or project; (b) include such copies in the archives and digital repositories of the University; and (c) make freely available such copies to third parties for research or educational purposes.

☑   I authorize the American University of Beirut, to: (a) reproduce hard or electronic copies of it; (b) include such copies in the archives and digital repositories of the University; and (c) make freely available such copies to third parties for research or educational purposes after: **One** ✓ **year from the date of submission of my thesis, dissertation or project.**
Two ___ **years from the date of submission of my thesis , dissertation or project.**
Three ___ **years from the date of submission of my thesis , dissertation or project.**

_____   8/2/2021____
        Signature   Date

This form is signed when submitting the thesis, dissertation, or project to the University Libraries

Acknowledgements

An Abstract of the Thesis of

Hassan Issa El Atwi   for   Master of Engineering
                              Major: Electrical and Computer Engineering

Title: Trajectory Tracking of Autonomous Vehicles via Model Predictive Control Aided by Sliding Mode Control

In this work, we propose a composite control system for stable and robust trajectory tracking of autonomous ground vehicles (AGVs) in the presence of bounded disturbances and uncertainties. A nominal model predictive control (MPC) system is combined with a sliding mode controller (SMC) to formulate the proposed control system under the umbrella of tube-based MPC approach, with the aim of tackling the trajectory tracking challenge for AGVs in uncertain environments. The control scheme is further modified by replacing the classical first-order sliding mode control (FOSMC) with a second-order one, the super twisting sliding mode controller (STSMC), to obtain a smooth control signal by diminishing the chattering phenomena. The proposed system's stability is analyzed and guaranteed via Input-to-State Stability (ISS) in coordination with Lyapunov stability theory.

For the first time, this combined control structure is applied to the nonlinear kinematic model of AGVs, where STSMC plays the role of an auxiliary controller in the feedback loop to handle disturbances and uncertainties that cause deviation from the nominal model. In particular, the auxiliary STSMC approach is used to produce a control action that reduces the difference between the nominal predicted states and the actual ones, with the main performance metric being the error between the vehicle's position and orientation against a desired trajectory, in addition to fulfilling all of the optimization constraints. A comparative simulation study is presented and demonstrates the effectiveness and robustness of the proposed composite control system in the presence of disturbance effects.

Contents

List of Figures

List of Tables

Chapter 1

Introduction

Self-driving vehicles are a transformative technological innovation in the mobility sector owing to their improved safety, accessibility, efficiency, and convenience in transportation. The last three decades have witnessed an increase in research efforts for the sake of developing driverless vehicle technology [2]. Autonomous vehicles are no more an illusion, they have already become a reality with autonomous vehicles able of tracking given paths [3]. Driverless cars are essentially autonomous decision-making systems that process a stream of observations from on-board sensors such as radars, LIDARs, cameras, GPS/INS units, and odometry [2], and send appropriate commands to actuators that induce the desired actions and motion.

A scale for grading vehicle's level of automation, which varies from 0 to 5, is introduced by SAE J3016 standard; vehicle automation grade vary from fully human operated (Level 0) to fully autonomous (Level 5) [4]. Based on a stream of observations from on-board sensors such as radars, LIDARs, cameras, GPS/INS units, and odometry, autonomous vehicle systems analyze data and make corresponding decisions [4]. Due to an autonomous system's increased reliability and faster reaction time as compared to human operators, the number of traffic collisions is expected to be drastically reduced upon the wide adoption of driverless vehicles. In addition, autonomy would also reduce traffic congestion, increase roadway capacity, reduce the need of safety gaps (e.g. platooning) and will lead to better traffic flow management [5]. Last but not least, autonomous vehicles can facilitate the transportation of people who are unable to drive due to physical or visual disability [6].

Autonomy can be generally divided into two sub-classes: perception and planning. In vehicles, perception is responsible for mapping the surrounding environment and localizing the vehicle within the generated map. On the other hand, planning is responsible for the decision making process that allows the vehicle to follow a desired trajectory while avoiding obstacles. The latter requires a global path planner for constructing an obstacle-free path from a chosen initial configuration to a goal configuration on an occupancy grid map that is provided by the

perception subsystem. Furthermore, a local motion planner that operates at a higher frequency continuously reconstructs the vehicle's local path and plans the its motion to avoid unexpected changes in the environment (for instance, avoiding dynamic obstacles) [7]. The desired motion is then translated into actuator commands on the vehicle's throttle, steering, and braking subsystems through an adopted vehicle model and dedicated controllers.

One of the most fundamental aspects of autonomous ground vehicles and mobile wheeled robots is optimal path planning and obstacle avoidance [8]. Motion planning entails finding collision-free paths in the configuration space, where various probabilistic and deterministic methods can be used to search for this path from the initial point to the goal point. Once the motion is planned, the trajectory planning stage takes into consideration the vehicle's constraints along this path such as maximum achievable acceleration and deceleration, and minimum turning radius. When the environment includes dynamic obstacles, time is considered as an additional constraint in the optimization problem. Finally, path planning is responsible for planning the path within the points generated by the motion planner. Usually operating at a higher frequency than the motion planner and in a 2D Euclidean space, the path planner is responsible for solving the problems that the motion planner could not tackle on a global level such as convex obstacles and unexpected static or dynamic obstacles. After discretizing the planners, the planned path and motion are fed to the vehicle model in order to produce the proper commands to the individual actuators: throttle, braking, and steering [9].

Autonomous ground vehicles comprise several subsystems that constitute fields of research on their own. Trajectory-tracking control is an active area of research that has benefited from noticeable contributions over the years [10]. Researchers have proposed various approaches to address the AGV tracking control challenge, which include geometrical approaches [11], backstepping [12], feedback linearization [13], sliding mode control [14], and model predictive control [15, 16], to only list a few. The main difficulties of the tracking control of mobile robots arise from their nonlinear dynamic models and underactuated configurations. Difficulties increase in ground vehicles since their motions must be planned while satisfying multiple physical constraints such as the nonholonomic constraint, velocity constraint, and input saturation constraint. As such, model predictive control has shown its effectiveness amongst other approaches due to its advantage of handling physical constraints, while simultaneously optimizing the control performance [17].

Robustness is another key feature that a motion control system must possess in order to yield acceptable tracking performance in the presence of uncertainties and disturbances. For the case of AGVs and mobile robots, several factors introduce uncertainties such as parametric uncertainties, measurement noise, unmodeled dynamics and nonlinearities, and external disturbances. To address this problem, researchers have proposed various robust control techniques, with the

majority being based on sliding mode control (SMC) or model predictive control (MPC), since the two schemes offer enhanced robustness against various disturbances. SMC is a suitable method for dealing with nonlinear uncertain systems, such as AGVs with nonholonomic constraints, and guarantees the elimination of matched disturbances [18]. SMC guarantees high performance under disturbances and uncertainties, albeit with a risk of subjecting the plant actuators to physical damage due to control signal chattering. Various approaches have been proposed to overcome the chattering effect such as high-order sliding mode controllers (HOSMC) and second-order sliding mode controllers (SOSMC). Another very effective scheme for dealing with chattering is the super twisting sliding mode controller (STSMC), which is a continuous SOSMC that generates smooth control signals that overcome the classical SMC drawbacks. Several control structures that offer robustness based on MPC exist in literature. Min-max formulation was first introduced in [19] to simply minimize the worst-case deviation from a specified reference. However, the min-max method suffers from drawbacks related to high computational cost and limited applicability to slow dynamics. A constraint tightening scheme, known as tube-based MPC (TMPC), was proposed to address the computational expense of the min-max approach. TMPC maintains the actual state within an invariant 'tube' around a nominal trajectory that is computed while neglecting disturbances [20], and it then forces all possible trajectories of the uncertain system to remain inside the tube boundaries [21]. The actual constraints are satisfied by replacing them with stricter ones in the optimization problem. TMPC consists of a dual control scheme, MPC with tightened constraints and an inner feedback loop to robustify the control system about the center of the designed tube [22, 23]. The effectiveness of both controllers, MPC and SMC, inspired several researchers to combine these two controllers in a single scheme to simultaneously benefit from both abilities [24].

In this work, we propose a tube-based MPC scheme for AGVs by augmenting a nominal MPC with STSMC in the feedback loop to improve trajectory tracking performance in the presence of uncertainties, which is achieved by the STSMC's robustness and the nominal MPC's ability to handle system constraints. This control scheme solves the trajectory tracking problem for AGVs and wheeled mobile robots by achieving minimum error while tracking a reference trajectory and fulfilling the control requirements from the viewpoints of stability, robustness, and no constraints violation.

The outline of this thesis is as follows: Chapter 2 presents a review of other related works available in the literature, which cover control schemes and solutions proposed to tackle the trajectory tracking problem of mobile ground robots. In Chapter 3, the perturbed nonholonomic nonlinear kinematic vehicle model is introduced and the proposed control system structure is described and formulated. The proposed control scheme is validated via numerical simulation in Chapter 4. A conclusion and an outlook into future work are provided in Chapter 5.

Chapter 2

Literature Review

This chapter reviews the major advances and main trajectory tracking methods that are available in the literature of mobile ground robots. First, geometrical approaches, which are simple to design and implement, are described. However, the tracking performance of AGVs using geometrical approaches is only guaranteed for low speeds. Next, several Lyapunov-based algorithms are discussed due to their widespread usage based on their guarantee of system stability. The chapter then discusses model predictive control (MPC) systems, which provide an optimal solution with the drawback of added computational cost, and they feature robustness and good performance in addition to stability guarantees. Detailed discussions of the pros and cons of the above approaches are presented in the respective sections.

2.1 Geometrical Approaches

Geometric controllers are widely common path tracking methods that are applied in mobile robots. These controllers benefit from the geometric relations between the vehicle's kinematics and the desired path, which result in direct control law solutions to the path-tracking problem [25]. The low computational requirement of geometrical approaches is considered their main advantage, given that they provide acceptable tracking performance [11]. The Pure Pursuit (PP) algorithm, illustrated in Fig. 2.1, is the most common and effective geometric method [26]. The PP algorithm computes a curvature that results in driving the vehicle to a chosen point on the path that is one look-ahead distance from the current vehicle position [11]. The look-ahead distance is the only parameter that needs to be tuned based on the vehicle's velocity, which makes the implementation of the PP algorithm relatively straightforward. If the magnitude of the look-ahead distance is small, the vehicle tends to oscillate about the desired path and can even become unstable for very small values [27]. On the other hand, longer look-ahead distances cause the vehicle to converge to the path more gradually

and with less oscillations; however, longer look-ahead distances cause the vehicle to short-circuit arced paths, thus the controlled vehicle cannot negotiate curvy maneuvers [28].

Stanley's method is another geometrical approach developed by the team at Stanford University and implemented on their vehicle "Stanley" for the DARPA Grand Challenge [29]. The velocity and steering controllers are applied separately; the steering angle is computed by a nonlinear feedback function of the cross-track error, while velocity control is implemented as a proportional-integral (PI) controller. The main shortcoming of the Stanley method is that its controller's performance degrades severely as the vehicle speed increases [30].

Figure 2.1: Pure pursuit algorithm.
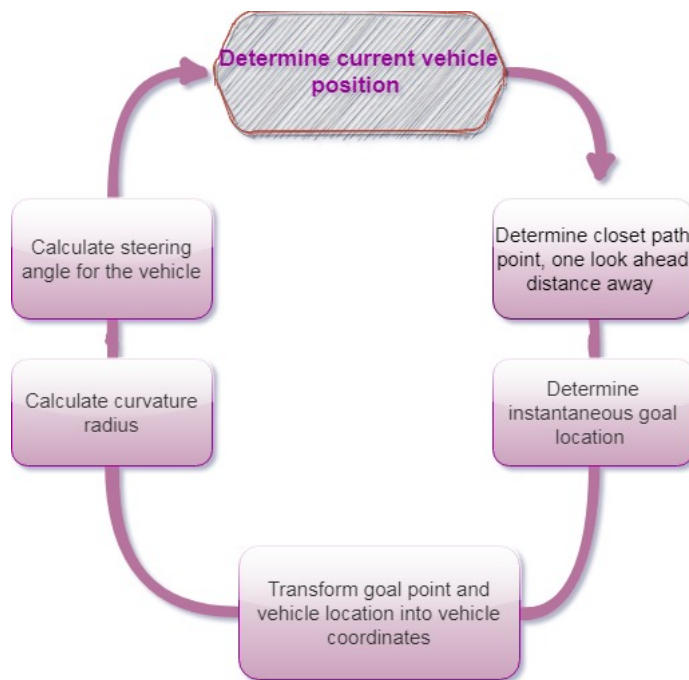
2.2 Lyapunov-Based Approaches

This section describes several Lyapunov-based controllers that are used for AGV tracking. These methods are widely implemented in various forms and aspects to achieve closed-loop stability. The following control algorithms are described in this section and covered in detail: feedback linearization, sequential backstepping, and sliding mode control.

2.2.1 Feedback Linearization

Feedback linearization is a Lyapunov-based method that has the advantage of transforming a nonlinear dynamic system into a linear one, which permits using linear control design techniques to address nonlinear closed-loop performance specifications [31]. Feedback linearization has been implemented in several applications in the robotics field. For instance, output feedback linearization was proposed in [32] to control a mobile ground robot with two arms. The proposed controller consisted of two components to achieve compatible and smooth motion between the arms and the base. The first part controls the orientation and the position of the base, Whereas the second part controls the manipulators for consistent behavior. A wheeled mobile cable-driven parallel robot was considered in [33]. Its mathematical equations were obtained via the Gibbs-Appel formula, then a linearized output feedback control law was designed. Simulations and experiments validated the performance of the proposed system. An adaptive controller was designed in [34] via sliding modes with feedback linearization for heavy deliveries by parachute from an airship; the controller's stability was achieved based on Lyapunov's theory, and validation was performed via numerical simulations.

2.2.2 Backstepping

Backstepping is a systematic control synthesis technique that divides a complex nonlinear system into several subsystems. It employs a recursive procedure that combines the choice of a Lyapunov function with the design of feedback control. The backstepping design starts from the system's lowest-order differential equation, introduces the concept of virtual control, and designs the virtual control inputs step-by-step to obtain the entire system's control law [35]. The recursive procedure of backstepping has attracted widespread attention to provide novel solutions for the trajectory tracking problem of mobile robots [35]. A backstepping control design for trajectory tracking of mobile robots was introduced in [36, 37]. The controller ensured global stabilization achievement, albeit under specific conditions and considering limits on velocities. To overcome the limitation in the previous work, a modified version was proposed in [38], but the computational effort of this scheme restricted its suitability for real-time implementation. A reduced-order backstepping controller was proposed in [39] by decoupling the two control inputs and adding an integral term for performance enhancement; the simplicity of the proposed controller makes it suitable for real-time experimentation.

2.2.3 Sliding Mode Control

Sliding mode control (SMC) is another effective method that deals with nonlinear uncertain systems and guarantees the complete elimination of the effects of

6

matched disturbances, which disturb a dynamic system through its input channel(s). The main aim of SMC design is to diminish the complexity of high-order systems to first-order state variables, namely the sliding function and its derivative. It offers high accuracy, robustness, fast response, easy tuning, and relatively simple design [40]. SMC is designed to drive and then constrain the system states to lie within the neighborhood of a particular surface in the state-space, named sliding surface (sliding function). After driving the states to the sliding surface, a selection of a switched feedback control law allows the states to remain on the surface [41]. SMC has been employed in solving tracking control problems of mobile robots [42, 43]. In [44], an adaptive sliding mode control with an extended state observer was presented to improve the trajectory tracking performance of a wheeled mobile robot under unknown skidding and slipping conditions.

A main concern with SMC laws is maintaining the states near the sliding surface, which may induce severe oscillations since SMC involves high frequency switching, which is known as the chattering phenomenon. Chattering is unacceptable since it reduces control accuracy, causes high heat losses in electrical circuits, and induces wear of mechanical parts [45]. Several methods that offer the elimination of chattering in SMC exist in literature, yet they can have an advantageous or deteriorative side effect on the controller's performance against disturbances. A simple way to avoid chattering is replacing the discontinuous signum function (sign) in the SMC control law with a continuous hyperbolic tangent function (tanh); however, this method tends to reduce the robustness feature of the controller against disturbances. The idea of reaching a delicate compromise between completely cancelling chattering and maintaining the robustness feature of SMC has motivated researchers to propose other controller enhancement methods. These enhancements can entail modifying the sliding surface such as integral SMC, fractional-order SMC, and terminal SMC [45]. High-order SMC (HOSMC) is another form of SMC design enhancement, where the control inputs act on higher derivatives of sliding surfaces, unlike FOSMC that deals with first-order derivatives only. HOSMC provides a smoother control signal, improved performance, and better chattering effect suppression in comparison to the FOSMC [46].

Second-order sliding mode (SOSMC) is a HOSMC algorithm that depends on setting both the sliding surface and its first derivative to zero. A significant challenge of SOSMC is the usage of derivatives in generating the control signal, which requires significant care in real-time implementation since it may cause severe oscillations in the presence of measurement noise. To overcome this issue, the super-twisting sliding mode control was introduced as a continuous SOSMC[47]. When compared to other SOSMC algorithms such as the twisting SMC, STSMC has a simpler control signal, provides continuous control laws, and it does not require the measurement of the first-order sliding surface derivative.

2.3   Model Predictive Control

Model predictive control (MPC), also known as receding horizon control (RHC), is widely used in industrial process control [48]. MPC is an optimal control method that uses the model of the process to predict and optimize the system response over a finite prediction horizon [49], while considering constraints on the system states and inputs. A significant concern with using a finite prediction horizon is to determine whether such a control action can guarantee system stability [50]. While it is shown that an infinite predictive horizon can guarantee the stability of a system, the choice of an infinite predictive horizon is not feasible for nonlinear systems in practice [15].

At each time step of the MPC algorithm, only the first step of the generated control sequence is applied to the plant [51]. Fig. 2.2 illustrates the MPC approach and shows how the receding horizon strategy introduces feedback. The various existing MPC algorithms differ among themselves in the model used to represent the plant, the noise representation, and the optimization algorithm to minimize the cost function [15]. MPC has been employed by researchers to deal with the trajectory tracking challenge of nonholonomic mobile robots [52, 53]. In [53], a robust nonlinear MPC (NMPC) was designed for the path following problem, where the initial value is determined online by the optimization problem, both recursive feasibility and stability were proven, and simulations confirmed the controller performance. In [17], five different trajectory tracking control approaches (Stanley, Linear Quadratic Regulation, SMC, Fuzzy Logic, and MPC) were applied to simulate an overtaking maneuver executed at 120 km/h. The results from the preliminary comparison (i.e., trajectory tracking and actuation) among the conducted controllers demonstrated that MPC resulted in the smallest tracking errors (i.e., lateral position and heading angle) with smooth actuation of the steering angle. In [54], two robust MPC schemes (TMPC and nonlinear MPC) were designed for tracking unicycle robots with input constraints and small bounded disturbances. Feedback linearization was used for designing the auxiliary controller in the TMPC framework. Input-to-State Stability (ISS) theory was leveraged to prove robust stability for both controllers. Both controllers exhibited effective performance, and less computational expense was recorded for the TMPC approach. Another MPC scheme for trajectory tracking of nonholonomic mobile robots was proposed in [55], where an adjusted cost function was adopted to minimize the distance between a given reference trajectory coordinate and the current robot pose. The proposed cost function includes a term that penalizes the distance between the next waypoint and the mobile robot. Simulation results show that the cost function modifications increased the algorithm's computational efficiency. To diminish the computational effort, a threshold for the error between the predicted and actual states in the event-based model predictive framework was introduced in [56], which helped solve the tracking control problem of nonholonomic systems in the presence of bounded disturbance.
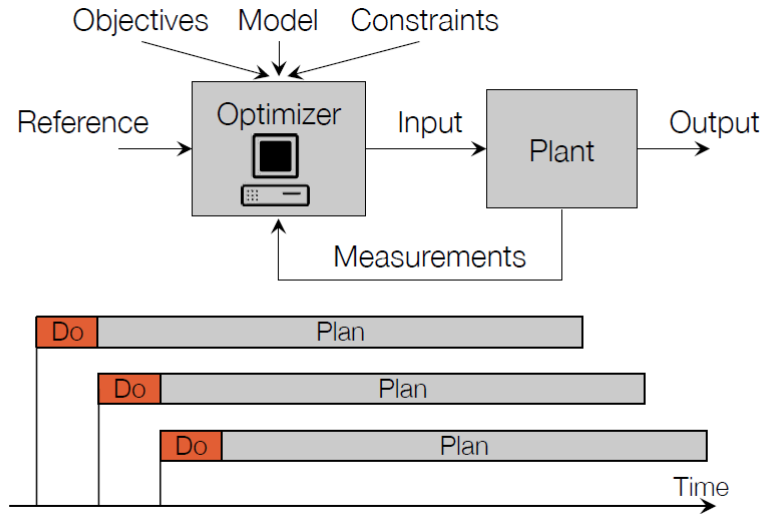
Figure 2.2: Model Predictive Control Scheme [1].

2.4 Robust Control

In addition to stability and performance, robustness is a critical feature that defines the effectiveness of a given control system. The level of required robustness depends on the magnitude of encountered disturbances and parametric uncertainties that affect the system under control. Robust control guarantees system stability and performance in the presence of uncertainties and disturbances, within certain known bounds [57]. Several factors introduce uncertainties in mobile robots and AGVs such as sensor measurement noise, unmodeled dynamics, external and internal disturbances, and parametric uncertainties [58]. To solve the challenging problem of trajectory tracking of mobile robots in the presence of large (yet bounded) disturbances and uncertainties, researchers have proposed various robust control schemes, with the majority being based on sliding mode control (SMC) [42, 43] or model predictive control (MPC) [52, 53], as will be detailed next.

2.4.1 Robust MPC

Robustness can be achieved through different control structures that are based on MPC. Benefiting from the essential advantage of MPC by computing a new control command online at each sampling time, some degree of robustness can be attained based on feedback control [59]. One method to deal with uncertainties is by considering the nominal disturbance-free system. This approach benefits from the advantage that MPC computes a new command at every sampling time, which aids in diminishing disturbances [60]; however, there is no guarantee for

9

achieving robustness without modeling the uncertainties in the control process. Another approach to resolve the robustness issue is the min-max formulation, which was first introduced by Campo and Morari [19]. The main aim of the min-max formulation is to minimize worst-case deviation, i.e. the uncertainty that maximizes the specified performance index, while guaranteeing constraint satisfaction for possible uncertainties. However, the min-max method has the drawbacks of high computational demand and it only applies to systems with slow dynamics. A new constraint tightening scheme, namely tube-based MPC, has been proposed to overcome the drawbacks of the min-max approach in terms of computational complexity.

Tube-Based MPC: When unknown but bounded uncertainties are present in a system, several future trajectories or possible solutions exist, each corresponding to a particular uncertainty. When introducing constraints in the optimization problem, the control objective becomes to satisfy the constraints in the presence of uncertainties. Hence, the main objective in tube-based MPC is to design a tube that maintains all possible trajectories of an uncertain system inside of it [21]. To guarantee that the actual constraints are satisfied, tube-based MPC replaces them with stricter ones in the optimization problem. Tube-based MPC consists of a dual control scheme, MPC with stricter tightened constraints and an inner feedback loop to further robustify the system about the center of the designed tube [22, 61]. The center of the tube is the trajectory of the uncertainty-free model generated by the nominal MPC [20].

Tube-based MPC (TMPC) was first introduced in [62] for linear time-invariant (LTI) systems with additive uncertainty. It was shown that the computational complexity is linear rather than exponential with the increase of prediction horizon. Researchers have introduced enhancements to the basic TMPC approach to make it handle nonlinear systems [63, 64, 65, 66]. A tube-based MPC scheme based on robust control invariant set, with application to Lipschitz nonlinear systems, was proposed in [66]. A similar formulation was used in [67] to control generic linear parameter-varying (LPV) systems, and in [68] to control the nonlinear dynamic model for an unmanned aerial vehicle (UAV).

Tube-based MPC has been employed to solve the trajectory tracking problem of mobile robots to guarantee stability, performance, and robustness. For instance, tube-based MPC was applied in [21] to the kinematic model of a mobile robot, in off-road conditions with longitudinal slip, to validate the performance and robustness of the tube-based MPC both experimentally and via numerical simulations, which offered a comparative analysis between TMPC, time-varying control techniques, and a slip effect compensator. Also, a robust positive invariant (RPI) set for tightening the constraints was designed in [69] to apply tube-based MPC to nonholonomic systems. The authors in [22] proposed a robust solution for the probing motion planning problem based on tube-MPC, where the probing

10

property was guaranteed by using the partially closed-loop strategy as a stochastic framework. TMPC was applied in [54] to control the motion of a mobile robot, where feedback linearization plays the role of the feedback controller that aids the TMPC system. Furthermore, a composite control scheme that consists of TMPC and adaptive control was proposed in [10] to handle both the kinematic and dynamic constraints of nonholonomic mobile robots.

2.4.2 Robust MPC-SMC Schemes

While several control structures that offer robustness based on MPC exist in the literature, researchers have also proposed to combine MPC with SMC in the feedback loop to ensure robustness. The motivation is to maintain the ability to explicitly deal with state and input constraints via MPC, while attaining increased robustness via SMC. This combination has been used in the literature in various ways and purposes. In [70], the latter combination was structured in a cascaded form, where MPC was used to update the sliding mode parameters to achieve certain performance objectives such as minimum energy or minimum time. Combining MPC with SMC also took the structure of a feedforward-feedback control scheme such as in [71, 72] where SMC was used as an auxiliary control law under the tube-based MPC approach. However, in [72], the nominal MPC that was used in [71] was substituted by another based on discrete-time Laguerre functions. In addition to that, an integral sliding mode (ISM) has been proposed instead of a full state feedback (FSF) controller integrated with MPC to control Continuous-time sampled-data nonlinear systems in [73]. The authors in [74] proposed to combine MPC and SMC in electrical grid applications, where simulation results showed the computational efficiency of this composite scheme over a conventional MPC by means of a significant reduction in the algorithm's execution time. For mobile robot applications, the MPC-SMC combination was used in [75] to control the lateral motion of a mobile robot using its linear time-invariant (LTI) dynamic model.

2.5 Thesis Contributions

The main contributions of this thesis compared to the existing trajectory tracking solutions in the literature are summarized next.

- Proposing a new robust control scheme for nonlinear systems using a composite framework that combines tube-based model predictive control (TMPC) and super twisting sliding mode control (STSMC).

- Providing a formal proof for the robust stability of the proposed composite scheme via Input-to-State Stability (ISS) and Lyapunov stability theorem.

11

- Implementing, for the first time, a tube-based MPC for the nonlinear kinematic model of an autonomous ground vehicle (AGV), with SMC playing the role of the auxiliary controller in the feedback loop. The proposed scheme is able to solve the trajectory tracking problem for AGVs and wheeled mobile robots by achieving minimum error while tracking a reference trajectory, in the presence of bounded disturbances and uncertainties, and fulfilling the control requirements from the viewpoints of stability, robustness, and no constraints violation.

Chapter 3

Proposed Control System Design

This chapter provides the design process of the proposed control system for trajectory tracking of AGVs in presence of disturbances and uncertainties. The nonlinear kinematic vehicle model is presented first. Then, the proposed composite control scheme is explained by further motivating the combination of MPC and STSMC in the tube-based MPC framework, which is followed by a detailed mathematical formulation of tube-MPC aided by SMC and STSMC. Finally, a formal proof of the proposed control system's robust stability is provided.

3.1 Nonholonomic Nonlinear Kinematic Model of Ground Vehicles

Consider a nonholonomic ground vehicle with perturbed input formulated by the following unicycle kinematics:

$$\dot{X} = f(X(t), u(t) + \Omega(t)) = \begin{bmatrix} [v(t) + dv(t)] \cos \theta(t) \\ [v(t) + dv(t)] \sin \theta(t) \\ \omega(t) + d\omega(t) \end{bmatrix}, \qquad (3.1)$$

where $X(t) = [x(t), y(t), \theta(t)]$ is the vector of Cartesian coordinates (x, y) of the vehicle's geometric center its heading angle (θ); $u(t) = [v(t), \omega(t)]$ is the vector of linear and angular velocities, respectively; and $\Omega(t) = [dv(t), d\omega(t)]$ represents the input disturbances.
The constraints on the allowable states are given by:

$$X \in \mathbb{X} = \{x \mid \Lambda x \leq \lambda\}, \qquad (3.2)$$

the constraints on the allowable input are given by:

$$u \in \mathbb{U} = \{u \mid \Delta u \leq \delta\}, \qquad (3.3)$$

and the constraints on the allowable range of disturbances are given by:

$$\Omega \in \mathbb{W} = \{w \mid Hw \leq \eta\}, \tag{3.4}$$

where Λ, Δ, and $H \in \mathbb{R}^n$.

Assumption 1 *Sets $\mathbb{X}$, $\mathbb{U}$, and $\mathbb{W}$ are polyhedral and convex, they are bounded and thus polytopic, they are of full dimension, and they contain the origin in their interior.*

3.2 Proposed Control Scheme

Trajectory tracking control of a nonholonomic mobile robot (NMR) aims at making the actual position and orientation of the NMR converge to a desired reference trajectory [10]. A key challenge in this tracking problem arises from internal and external disturbances that influence the robot dynamics and from uncertainties in sensing and control signals, which diminish the ability to satisfy the system states and inputs constraints, nonholonomic motion constraints, and collision avoidance constraints. As mentioned in Chapter 2, several control system designs have been proposed to achieve the requirements of the trajectory tracking problem. However, the majority of the available techniques are unable to ensure the fulfillment of constraints and performance against uncertainties at the same time and within the same accuracy level. Experimental results and real-time implementation emphasize the ability of SMC to deal with uncertainties, and the effectiveness of MPC to handle the system constraints. Hence, the combination of MPC and SMC is expected to enhance the system's ability to track reference trajectories in the presence of uncertainties and disturbances, while respecting the constraints on the states, inputs, and motion.

However, a main concern with MPC remains its computational expense given the requirement of having to solve an optimization problem online. On the other hand, the computational expense of SMC is relatively minimal, which makes it suitable as an auxiliary controller in the feedback loop within a TMPC scheme. To speed up the computation and reduce complexity, a nominal MPC is designed to control a nominal plant model, which comes at the cost of a compromised disturbance rejection ability. This further motivates the employment of SMC in the feedback loop to offer disturbance rejection with minimal additional computational effort. The resultant control system is a two-degrees-of-freedom controller, where MPC provides model-based feedforward control and SMC generates feedback control to compensate for the deviation between the real and nominal system, even in the presence of disturbances and uncertainties that are not handled by the nominal MPC.

But before implementing SMC as an auxiliary aid to the nominal MPC, we must account for SMC's undesirable chattering that can be detrimental to the
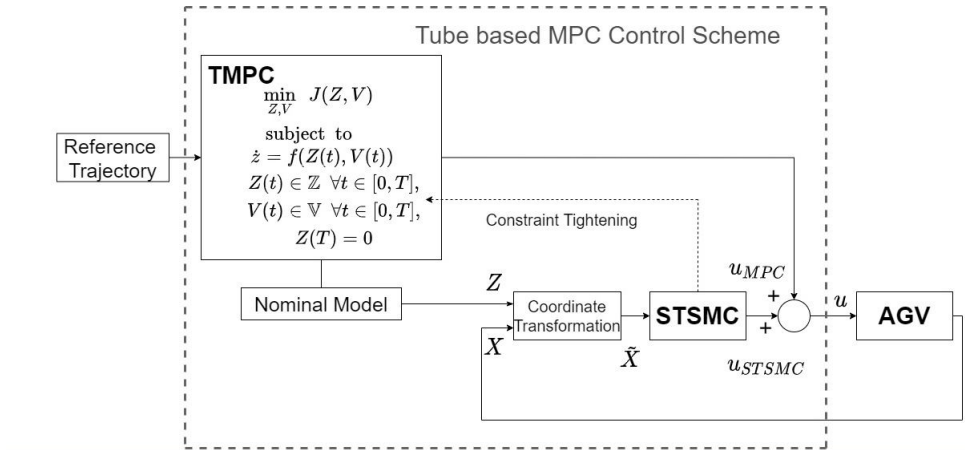
Figure 3.1: A block diagram of the proposed composite control system. The MPC system generates a control signal (u_{MPC}) based on the optimization of a cost function that considers the error between the nominal model states and the desired trajectory. The STSMC system generates a control signal (u_{STSMC}) based on the error between the nominal model states and the actual plant (AGV) states as measured by on-board sensors or estimated by observers.

control system performance. Chattering mainly stems from the presence of the so-called parasitic or unmodelled dynamics, which induce deviations that cause SMC to keep oscillating about the sliding surface. Second-order sliding mode control (SOSMC) systems are designed to help in eliminating the chattering effects by having both the sliding surface and its first derivative at zero, which theoretically results in chattering suppression and thus a smoother control signal. However, the drawback of using derivatives to generate the control signal in SOSMC presents a technical challenge in real-time implementation due to the presence of sensor measurement noise. To overcome this drawback of SOSMC, the super-twisting sliding mode control (STSMC), which is a continuous SOSMC, is employed as the auxiliary controller in the tube-based MPC scheme. STSMC has a simpler control algorithm as compared with other SOSMC systems, it provides a continuous control law, and it does not require the measurement of the time derivative of the SMC manifold.

Two cases are considered in the problem formulation, the first one is designing the TMPC with the classical first-order SMC (FOSMC), and the second one is substituting the FOSMC by the super-twisting sliding mode algorithm to validate its ability in eliminating the chattering phenomena. The control scheme is illustrated in Fig. 3.1, whereby the trajectory of the uncertainty-free model is generated by the nominal MPC's input, whereas the STSMC input deals with the deviation between the real and nominal states in the presence of disturbances and uncertainties.

The system state is split into two components: a nominal component, Z, and

a deviation from nominal, $\tilde{X}$, such that:

$$X = Z + \tilde{X}. \tag{3.5}$$

Given the aim of this work, the input is split into the input from the nominal MPC, u_{MPC}, and the input from the auxiliary STSMC, u_{STSMC}, such that:

$$u = u_{MPC} + u_{STSMC}. \tag{3.6}$$

3.3   Tube-based Model Predictive Control

Consider the nominal nonlinear kinematic model of a ground vehicle as:

$$\begin{cases} \dot{x}(t) = v(t) \cos \theta(t), \\ \dot{y}(t) = v(t) \sin \theta(t), \\ \dot{\theta}(t) = \omega(t), \end{cases} \tag{3.7}$$

where x and y are the Cartesian coordinates of the vehicle's geometric center, v is the translational velocity, θ is the heading angle, and ω_r is the angular velocity. Vector, $Z = [x, y, \theta]$, represents the system's nominal states and vector, $V = [v, \omega]$, is the control input generated by the nominal MPC (u_{MPC}). As a result, the following optimization problem is solved at each iteration:

$$\begin{aligned} &\min_{Z,V} \quad J(Z,V) \\ &\quad subject\ to \\ &\dot{z} = f(Z(t), V(t)) \\ &Z(t) \in \mathbb{Z} \quad \forall t \in [0, T], \\ &V(t) \in \mathbb{V} \quad \forall t \in [0, T], \\ &Z(T) = 0, \end{aligned} \tag{3.8}$$

where T is the prediction horizon, and $J(\mathbf{Z},\mathbf{V})$ is the cost function that has to be minimized and is given by:

$$J(Z,V) = \int_{t_k}^{t_k+T} L(Z(\tau|t_k), V(\tau|t_k))\, d\tau + g(Z(t_k + T|t_k)). \tag{3.9}$$

$L(Z(\tau|t_k), V(\tau|t_k)) = \|Z(\tau|t_k)\|_Q^2 + \|V(\tau|t_k)\|_R^2$ represents the cost function that penalizes the control effort and the difference between the current vehicle's pose and the reference trajectory, where the penalizations are associated with the weight matrices, Q=diag$\{q_1, q_2\}$ and R=diag$\{r_1, r_2\}$, which define the proportion of penalization over the cost function's global value. $J(\mathbf{Z},\mathbf{V})$ contains a quadratic function $g(Z(t_k + T|t_k)) = \frac{1}{2}\|Z(\tau|t_k)\|_P^2$, which is a terminal penalty

that guarantees stability when there exists a matrix $P > 0$. Furthermore, condition $Z(T) = 0$ in (3.8) imposes a terminal condition to ensure stability [23].

Hence, the nominal MPC computes the optimal trajectories with stricter constraints than the original ones in (3.2) and (3.3) given that it considers a disturbance-free model. Therefore, new sets of tighter constraints, $\mathbb{Z} \subset \mathbb{X}$ and $\mathbb{V} \subset \mathbb{U}$, are generated by means of the constraints tightening approach that is illustrated next in Section 3.3.1.

3.3.1 Constraints Tightening

An important feature of MPC is its ability to consider the constraints of a control problem in a relatively straightforward manner, a feature that should be preserved. However, minimizing the computational requirements by solving the nominal MPC problem and introducing an auxiliary SMC comes at the cost of losing this important feature, which is due to the fact that the proposed combination does not guarantee the satisfaction of the problem constraints. This poses a challenge that must be solved to overcome this potential drawback of the proposed control scheme; the solution is realized by modifying the MPC formulation. The MPC's original control constraints are modified by calculating an upper bound for the control input generated by SMC [24, 76], which is computed based on the trajectory tracking error boundaries given by:

$$Z - |\tilde{X}| \leq X \leq Z + |\tilde{X}|, \tag{3.10}$$

where Z is the nominal state trajectory, $\tilde{X}$ is the trajectory tracking error, and X is the real state trajectory. After obtaining the upper bound of SMC, the new input constraint is given by:

$$\mathbb{V} = \mathbb{U} - \mathbb{U}_{upper}, \tag{3.11}$$

where $\mathbb{U}$ is the set of original control constraints and $\mathbb{U}_{upper}$ is the upper bound of the SMC signal.

3.3.2 Adding an Obstacle as a Path Constraint

MPC provides the ability of avoiding obstacles while tracking a predefined trajectory by including additional constraints in the optimization problem. To avoid obstacles, the vehicle must maintain a lower-bound of the Euclidean distance between the prediction of its position and that of the obstacle. Thus, the following path constraint is imposed:

$$\sqrt{(x - x_o)^2 + (y - y_o)^2} \geq r_v + r_o, \tag{3.12}$$

where (x_o, y_o) is the obstacle position, and r_v and r_o are the radii of virtual circles that are placed around the vehicle and obstacle(s), respectively.

3.4 Auxiliary Control Based on Super-Twisting Sliding Mode Control

3.4.1 Sliding Mode Control

The sliding mode controller plays its auxiliary role in the feedback loop of the proposed scheme to compensate for the deviation between the real and the nominal states. SMC is designed based on the ground vehicle's nominal nonlinear kinematic model in (3.7). The deviation model between the actual system and the nominal system is given by the following trajectory tracking error vector:

$$
\begin{bmatrix} x_e \\ y_e \\ \theta_e \end{bmatrix} = \begin{bmatrix} \cos\theta_d & \sin\theta_d & 0 \\ -\sin\theta_d & \cos\theta_d & 0 \\ 0 & 0 & 1 \end{bmatrix} \begin{bmatrix} x_r - x_d \\ y_r - y_d \\ \theta_r - \theta_d \end{bmatrix},
\tag{3.13}
$$

where Fig. 3.2 shows the tracking error and the virtual vehicle pose that represents the reference pose (x_d, y_d, θ_d) at each sample time.
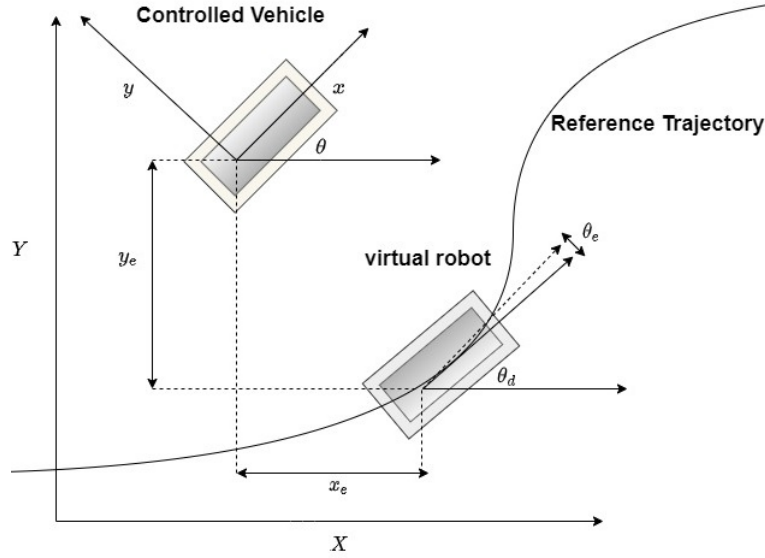
Figure 3.2: Tracking Error between the Controlled and Virtual Vehicles

The corresponding tracking error derivatives are:

$$
\begin{cases} \dot{x}_e = -v_d + v_r \cos\theta_e + y_e \omega_d, \\ \dot{y}_e = -v_r + v_r \sin\theta_e + x_e \omega_d, \\ \dot{\theta}_e = \omega_r - \omega_d, \end{cases}
\tag{3.14}
$$

where v_d and ω_d are the desired linear and angular velocities, respectively. The lateral error, y_e, and angular deviation, θ_e, are internally coupled with each other,

thus only two sliding surfaces are designed. The first surface, s_1, controls the convergence of x_e, while the second surface, s_2, controls the convergence of both y_e and θ_e. To reduce chattering, the sliding mode control action is smoothed by defining a boundary layer with thickness Φ around the switching surface using the saturation function instead of the signum function [24], as expressed below:

$$s_1 = \dot{x}_e + k_1.x_e, \tag{3.15}$$

$$s_2 = \dot{y}_e + k_2.y_e + k_0 sat(y_e/\Phi)\theta_e, \tag{3.16}$$

where k_0, k_1, and k_2 are positive constant parameters that are tuned per the desired performance requirements, and sat is the saturation function.

In SMC, there is a reaching phase that drives the system states towards a designed sliding surface. The exponential reaching law is given by:

$$\dot{s} = -\tilde{Q}s - \tilde{P}sat(s/\Phi), \tag{3.17}$$

such that $-\tilde{Q}s$ is an exponential term, where $\tilde{Q} = diag\{\tilde{q}_1, \tilde{q}_2\}$ and $\tilde{P} = diag\{\tilde{p}_1, \tilde{p}_2\}$ are constant positive definite matrices. After mathematical manipulation and adopting the reaching law in [77], the following equations that govern the control input formulation are attained:

$$\dot{v}_c = -\tilde{q}_1.s_1 - \tilde{p}_1.sat(s_1/\Phi) - k_1.\dot{x}_e - \dot{\omega}_d.y_e - \omega_d.\dot{y}_e + v_r.\dot{\theta}_e.\sin\theta_e + \dot{v}_d)/\cos\theta_e, \tag{3.18}$$

$$\omega_c = \omega_d + \frac{-\tilde{q}_2.s_2 - \tilde{p}_2.sat(s_2/\Phi) - k_2.\dot{y}_e - \dot{v}_r.\sin\theta_e + \dot{\omega}_d.x_e + \omega_d.\dot{x}_e}{v_r.\cos\theta_e + k_0.sat(y_e/\Phi)}, \tag{3.19}$$

where $\dot{v}_c$ is the linear velocity rate that is integrated to obtain the first control input, and w_c is the angular velocity and the second control input to the system.

3.4.2 Super-Twisting Sliding Mode Control

In this section, the proposed control system is modified by replacing the standard sliding mode control(SMC) with the super-twisting sliding mode control (STSMC) to play the role of the auxiliary controller in the composite scheme. The main drawback of the standard first-order sliding mode control system is chattering in the commanded control signal, where the modification aims to diminish this effect by generating a smooth control signal. As already mentioned in Chapter 2, STSMC is a second-order sliding mode control that forces both the sliding surface and its first derivative to zero in finite time. The super-twisting sliding mode control has an advantage over other second-order sliding mode controllers since it maintains the main properties of FOSMC, without a need for the derivatives of the sliding surface. The design process of the STSMC system is divided into two steps. First, the sliding surfaces are designed to capture the desired performance requirements. The second step is designing a control input to

ensure that the states stay on the designed surface [46]. The STSMC controller is designed based on the nominal nonholonomic vehicle model (3.7) and the error dynamic system (3.13). The corresponding error derivatives are given by:

$$\begin{cases} \dot{x}_e = -v_d + v_r . \cos \phi_e + y_e . \omega_d, \\ \dot{y}_e = -v_r + v_r . \sin \phi_e + x_e . \omega_d, \\ \dot{\phi}_e = \omega_r - \omega_d, \end{cases} \tag{3.20}$$

where v_d and ω_d are the desired linear and angular velocities, respectively. Similar to the standard FOSMC, it is sufficient to design only two sliding surfaces for the problem of AGV trajectory tracking, since the lateral error, y_e, and angular variable, ϕ_e, are internally coupled with each other. Therefore, the lateral dynamics error require only one surface (S_1) to obtain convergence, while the other surface (S_2) is designed for the longitudinal error.

$$S_1 = k_1 e_x + \int e_x dt, \tag{3.21}$$

$$S_2 = \dot{e}_y + k_2 e_y + k_3 sin(e_\theta) + \int e_y dt. \tag{3.22}$$

Integral terms are added to the sliding surfaces, which helps in achieving a zero steady-state error. The continuous control signal of STSMC that guarantees the convergence of S and $\dot{S}$ in finite time is given by:

$$V = -a_v \sqrt{|S_1|} \arctan (S_1) + \Upsilon, \tag{3.23}$$

$$\dot{\Upsilon} = -b_v \arctan (S_1), \tag{3.24}$$

$$W = -a_W \sqrt{|S_2|} \arctan (S_2) + Q, \tag{3.25}$$

$$\dot{Q} = -b_W \arctan (S_2), \tag{3.26}$$

where the virtual inputs Z and Q are used to get a smooth continuous control signal; V and W are the vehicle's linear and angular velocities, respectively. On the other hand, the controller gains a_v, b_v, a_W and b_w are positive and must satisfy certain conditions to guarantee stability, which are explained in Section 3.5.

20

3.5 Robustness and Stability Analysis

3.5.1 Input-to-State Stability (ISS) Definitions

This section deals with the stability analysis of the tube-based MPC aided by the super-twisting SMC for the uncertain nonlinear kinematic vehicle model. The framework used for the analysis of the robust stability of systems controlled by MPC is based Input-to-State Stability (ISS) theory. We first introduce the following closed-loop system:

$$\dot{x} = f(x(t), u(t) + d(t), w(t)), \tag{3.27}$$

where $x \in \mathbb{R}^n$ is the system state, u is the control signal $u \in \mathbb{R}^m$, $d \in \mathbb{R}^q$ is the matched disturbance (enters through the input channel), and $w \in \mathbb{R}^p$ is the unmatched disturbance (state dependent). The nominal model of the plant (3.27) denotes the system considering zero-disturbance, and it is given by:

$$\dot{\tilde{x}} = \tilde{f}(\tilde{x}(t), u(t)), \tag{3.28}$$

Definition 1: The system $\dot{\tilde{x}} = \tilde{f}(\tilde{x}(t))$ is globally asymptotically stable if there exist a KL function β such that $|\tilde{x}(t, |x(0)|)| \leq \beta(|x(0)|, t)$.

Definition 2: System (3.28) has an asymptotic gain if there exists a K function γ_a such that for each $x(0)$ and d, the state of the system satisfies the following property:

$$\limsup_{t \to \infty} |x(t, x(0), d)| \leq \gamma_a(\limsup_{t \to \infty} |d(t)|) \tag{3.29}$$

According to the above definitions of nominal stability and asymptotic gain, we can prove that the system is input state stable (ISS) as given next. System (3.27) is ISS if there exists a KL function, β, and a K function, γ, such that for all initial state $x(0)$ and disturbances d,

$$|x(t, x(0), d)| \leq \beta(|x(0)|, t) + \gamma(\|d\|). \tag{3.30}$$

The definition of input-to-state stability of a system comprises both effects: nominal stability and uniformly bounded effect of the uncertainties, in a single condition. Therefore, considering system (3.27), the nominal system is asymptotically stable (AS) and the disturbed system has an asymptotic gain (AG) [78], which means that it is indeed input-to-state stable (ISS).

3.5.2 TMPC-STSMC Robust Stability Analysis

This section presents the robust stability analysis of the proposed composite controller to deal with the trajectory tracking problem of ground vehicles and mobile robots in the presence of bounded uncertainties and disturbances. The input-to-state stability is considered a suitable framework for robust stability analysis. According to the definitions mentioned in the previous section for ISS theory, the first step of the robust stability analysis is to prove that the tracking error of the nominal model converges to the origin. Then, it should be shown that the real states converge to an invariant set along the nominal optimal trajectory, which is the center of the designed MPC tube. To demonstrate nominal stability, Lyapunov stability theory is used by choosing the cost function in the MPC formulation as a candidate Lyapunov function. Thus, the candidate Lyapunov function is $V_2 = J(Z^*, V^*)$.

Consider the difference of the Lyapunov function at t_k and t_{k+1}:

$$
\begin{aligned}
\Delta V_2 &= V_2(t_{k+1}) - V(t_k) \\
&\leq J(Z^*(t_{k+1}), V^* t_{k+1}) - J(Z^*(t_k), V^* t_k) \\
&= \int_{t_{k+T}}^{t_{k+1}+T} \|(Z(\tau|t_{k+1})\|_Q^2 + \|V(\tau|t_{k+1})\|_R^2 d\tau \\
&\quad - \int_{t_k}^{t_k+T} \|(Z(\tau|t_k)\|_Q^2 + \|V(\tau|t_k)\|_R^2 d\tau \\
&\quad + \|Z(t_{k+1}+T|t_{k+1})\|_R^2 - \|Z(t_k+T|t_k)\|_R^2, \\
&= -\int_{t_k}^{t_k+T} \|(Z(\tau|t_k)\|_Q^2 + \|V(\tau|t_k)\|_R^2 d\tau \\
&\quad + \int_{t_{k+T}}^{t_{k+1}+T} \|(Z(\tau|t_{k+1})\|_Q^2 + \|V(\tau|t_{k+1})\|_R^2 d\tau \\
&\quad + \|Z(t_{k+1}+T|t_{k+1})\|_R^2 - \|Z(t_k+T|t_k)\|_R^2.
\end{aligned}
\tag{3.31}
$$

The following inequality is defined for the nominal tracking error system, which is a compatibility condition between L and g to ensure stability [54]:

$$
\dot{g}(Z(t_k+T|t_k)) + L(Z(\tau|t_k), V(\tau|t_k)) \leq 0.
\tag{3.32}
$$

By integrating (3.32) from (t_k+T) to $(t_{k+1}+T)$, it follows that:

$$\|Z(t_{k+1} + T|t_{k+1})\|_R^2 - \|Z(t_k + T|t_k)\|_R^2$$

$$+ \int_{t_k}^{t_k+T} L(Z(\tau|t_k), V(\tau|t_k))\, d\tau \leq 0. \tag{3.33}$$

Substituting (3.33) into (3.32), we get that $\Delta V_2 \leq 0$, which implies that the nominal system is asymptotically stable and the nominal states are bounded by a class KL function, $\beta(.,.)$, such that:

$$\|Z(t)\| \leq \beta(\|Z(t_0)\|, t), \forall t > t_0. \tag{3.34}$$

Now, the stability of the super-twisting sliding mode control system must be guaranteed to validate that the error between the real states and the nominal states is bounded, and that the real states will indeed converge to the nominal trajectory. Consider the perturbed control signal generated by the super-twisting sliding mode algorithm as follows:

$$V = V_{STSMC} + \varrho_1, \tag{3.35}$$
$$\dot{\Upsilon} = \dot{\Upsilon}_{STSMC} + \varrho_2,$$

where the disturbance terms, ϱ_1 and ϱ_2, are globally bounded by:

$$|\varrho_1| \leq \eta_1 |S_1|^{1/2},$$
$$|\varrho_2| \leq \eta_2, \tag{3.36}$$

for some constants $\eta_1, \eta_2 \geq 0$.

To guarantee the robust stability of the closed-loop system, the following candidate Lyapunov function is considered to prove the stability of the STSMC algorithm:

$$V_3 = 2b_v |S| + \frac{1}{2}\Upsilon^2 + \frac{1}{2}(a_v |S|^{1/2} \arctan(S) - \Upsilon). \tag{3.37}$$

The proposed Lyapunov function (3.37) guarantees that the trajectory tracking error is bounded having chosen the gains in the STSMC algorithm to satisfy the following inequalities [79]:

$$a_v > 2\eta_1,$$
$$b_v > a_v \frac{5\eta_1 a_v + 6\eta_2 + 4(\eta_1 + \eta_2/a_v)^2}{2(a_v - 2\eta_1)}. \tag{3.38}$$

The proposed Lyapunov function can be written in the form $V_3 = \zeta^T P \zeta$, where $\zeta^T = [|S|^{1/2} sign(S), \Upsilon]$. Therefore, its time derivative is given by:

$$\dot{V}_3 = -\frac{1}{|S|^{1/2}} \zeta^T Q \zeta + \frac{\varrho_1}{|S|^{1/2}} q_1^T \zeta + \varrho_2 q_2^T \zeta, \tag{3.39}$$

where

$$q_1^T = \left[(2b_v + \frac{a_v^2}{2}) \quad -\frac{a_v}{2} \right] \quad q_2^T = \left[-a_v \quad 2 \right] \tag{3.40}$$

Given the bounds on the disturbances in (3.36),

$$\dot{V}_3 \leq \frac{1}{|S|^{1/2}} \zeta^T \tilde{Q} \zeta, \tag{3.41}$$

where

$$\tilde{Q} = \frac{a_v}{2} \begin{bmatrix} 2b_v + a_v^2 - (\frac{4b_v}{a_v})\eta_1 - 2\eta_2 & -(a_v + 2\eta_1 + \frac{2\eta_2}{a_v}) \\ -(a_v + 2\eta_1 + \frac{2\eta_2}{a_v}) & 1 \end{bmatrix}. \tag{3.42}$$

If the inequalities in (3.38) exist, then $\tilde{Q} > 0$, which implies that $\dot{V}$ is negative definite. As a result, the super-twisting sliding mode control algorithm is asymptotically stable, which means that the deviation between the nominal states and the real one is bounded, and there exists a K function $\gamma(.)$ such that:

$$\|\tilde{X}(t)\| \leq \gamma(\eta), \forall t > t_0, \tag{3.43}$$

where η is the upper bound of the disturbance.

It follows from (3.5), which splits the real states into nominal states and deviation from the nominal states, that:

$$\|X(t)\| \leq \beta(\|X(t_0)\|, t) + \gamma(\eta), \tag{3.44}$$

which indicates that the closed-loop system is indeed ISS.

Chapter 4

Simulation Results and Discussion

In this section, we provide a performance check of the proposed control system (MPC+STSMC) and compare it against the nominal MPC system to validate the robustness feature of the proposed controller. Furthermore, the two proposed auxiliary controllers (SMC/STSMC) are compared in terms of the smoothness degree of their control signals. Simulations are carried out in MATLAB using the CasADi toolbox [80], which is used to solve the optimization problem of the nominal MPC. The numerical simulations are conducted using an Intel Core i7-5500U @ 2.40 GHz processor, whereby comparing the loop-times of the nominal MPC ($2.58s$) and the proposed system ($2.96s$) reveals an improved performance at a reasonable computational cost increase of $\approx 15\%$.

The perturbed vehicle model is tested among several standard paths for validating the trajectory tracking controllers. The robustness attribute is verified by checking the performance against two types of disturbances: matched and unmatched. The matched disturbance is one that comes through the input channel. Matched Disturbance describes disturbances and uncertainties such as the delay between the high-level control that generates the linear and angular velocities (TMPC/STSMC) and the low level control that controls the vehicle actuators. On the other hand, the state-dependent disturbances are considered unmatched. The latter accounts for several categories of disturbance, such as road nature uncertainties(bumps, inclined surfaces) and measurement noise uncertainties. Several simulation scenarios are considered to confirm the ability of the proposed controller to achieve acceptable performance.

The original input and state constraints are respectively defined as follows: $\mathbb{X} = \{x, y \mid |x| \leq 100m \; ; \; |y| \leq 100m\}$ and $\mathbb{U} = \{v, \omega \mid |v| \leq 5m/s \; ; \; |\omega| \leq \pi/3rad/s\}$. The MPC parameters are set as follows: $N = 8$, $Q = diag\{1, 1, 0.5\}$, $R = diag\{0.5, 0.05\}$, $P = diag\{0.5, 0.5, 0.5\}$; and the SMC parameters are tuned as follows: $\tilde{Q}=diag\{2, 0.8\}$, $\tilde{P}=diag\{0.5, 0.5\}$, $k_0 = 1$, $k_1 = 5$, $k_2 = 6$, and $\phi = 1.2$. The tuned gains for the super twisting sliding mode control algorithm are as follows: $k_1 = 2$, $k_2 = 1$, $k_3 = 2$,$a_v = 5$, $b_v = 3$, $a_w = 5$, $b_w = 0.1$. In all scenarios, the disturbances are injected at 65 seconds. The first vehicle reference trajectory (sinusoidal) is generated as follows:

$$\begin{cases} x(t) = t, \\ y(t) = \sin 0.5t + 0.5t. \end{cases} \tag{4.1}$$

4.1 Disturbance-Free Scenario

In this section, the ground vehicle performance is tested without disturbance injection. Fig. 4.1 shows the trajectory tracking performance of the proposed control law for both cases (TMPC+SMC) and (TMPC+STSMC) versus the nominal MPC,SMC,and Lyapunov based controller designed in [81]. As observed, the tracking error is zero for all cases, and the mobile robot is able to follow the predefined path

Fig. 4.2 demonstrates the ability of the (TMPC+STSMC) system in obtaining a minimum tracking error. Despite considering a disturbance-free scenario, SMC results in a tracking error ,seen in Fig. 4.2, which is due to the noisy signal generated by SMC as shown in Fig. 4.4. On the other hand, we notice that chattering is avoided by the STSMC algorithm, as observed in Fig. 4.3, where no control effort is provided by STSMC in the absence of disturbances.

In contrast, the tracking error alone is not sufficient to demonstrate the superiority of one controller over another. Looking at the nature of the control input signal of each controller can give more insight about the inner workings of each design. Fig. 4.3 and Fig. 4.4 show the linear (right) and angular (left) velocities for both designs, and they demonstrate the advantages of using STSMC in terms of providing a smooth signal to the robot actuators. On the other hand, Fig. 4.4 shows significant chattering in the control signal of the SMC, especially at the beginning of the simulation, which is in contrast with the smooth STSMC signals. Another important aspect that these figures show is the role of both controllers
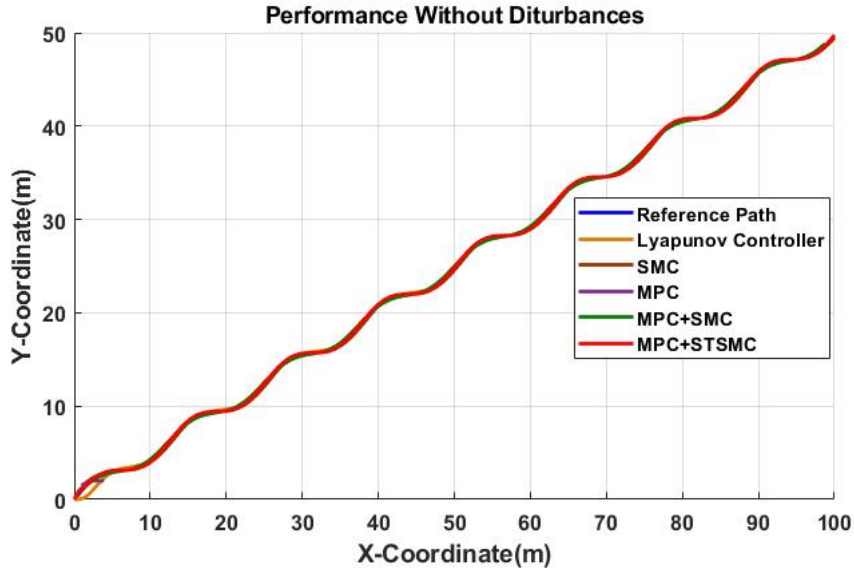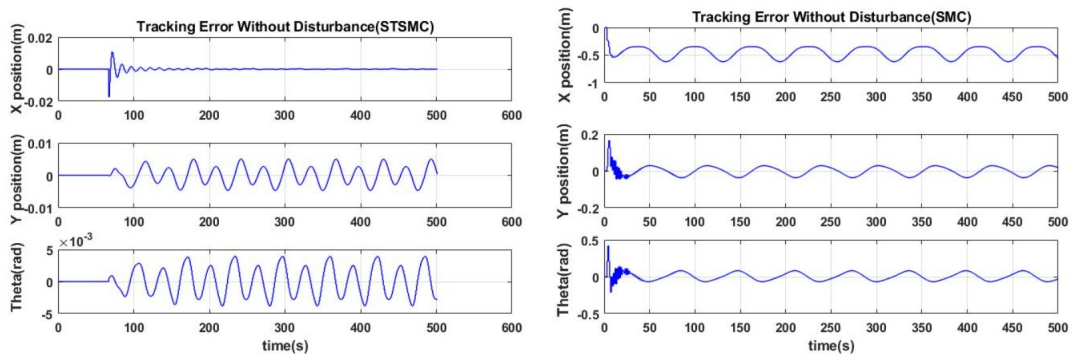
26

Figure 4.1: Trajectories without Disturbance

Figure 4.2: Tracking error without disturbance. Left: (TMPC+STSMC), Right: (TMPC+SMC)

in aiding MPC; it can be seen that their control signals remain near zero, which is consistent with the role of SMC in the proposed control as feedback controllers, in the sense that SMC does not contribute much to the total control effort in the absence of disturbances acting on the ground vehicle.

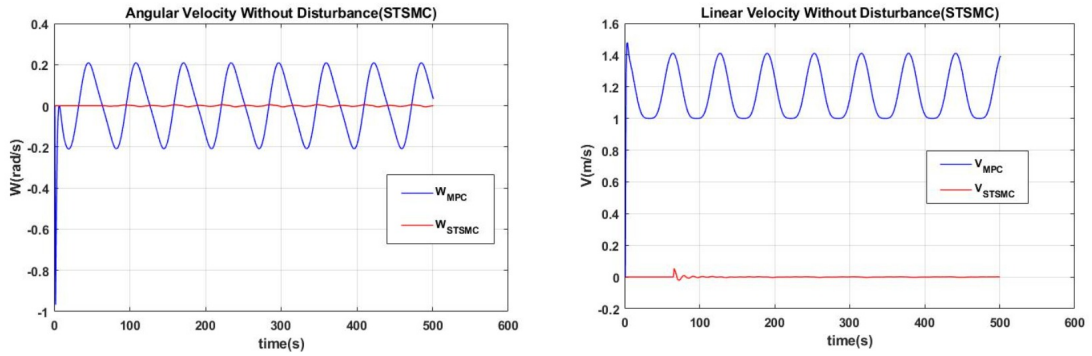Furthermore, Fig. 4.5 shows the ability of the (TMPC+STSMC) controller

27

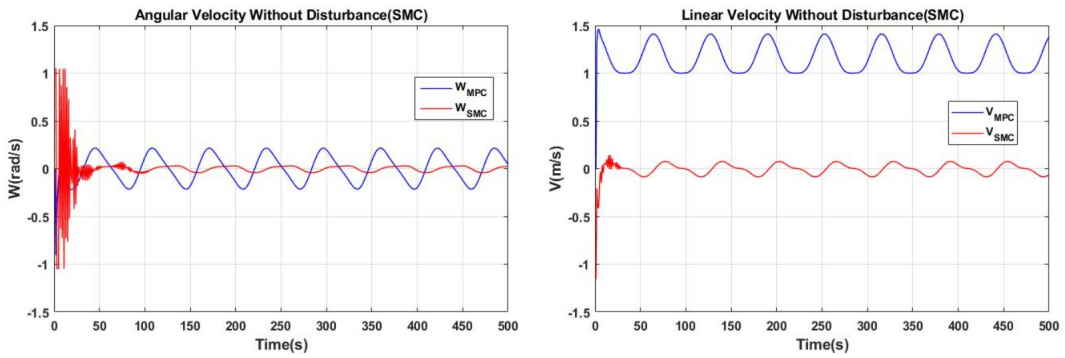Figure 4.3: Control Inputs Without Disturbance (STSMC)

Figure 4.4: Control Inputs Without Disturbance (SMC)

to satisfy the original constraints and remain within their specified bounds at all times, whereas the (TMPC+SMC) system results in constraint violation, exceeding both the upper and lower bounds of the rotational velocity, due to chattering.

Fig. 4.6 further demonstrates the advantage of using the STSMC algorithm, which maintains the sliding surfaces near zero at all times, whereas the SMC system does not drive the first sliding surface to converge to zero. These results indicate that STSMC can attain a smoother response in contrast to the SMC algorithm. The variation in SMC sliding surfaces, as shown in Fig. 4.6, is induced by chattering.
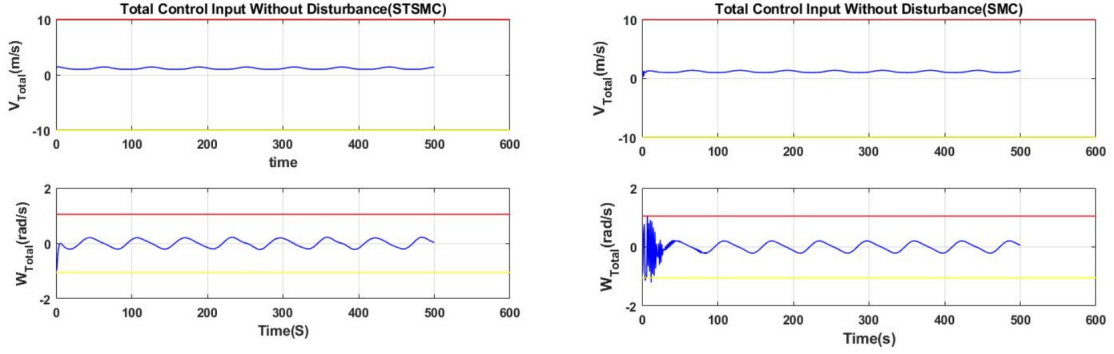
28

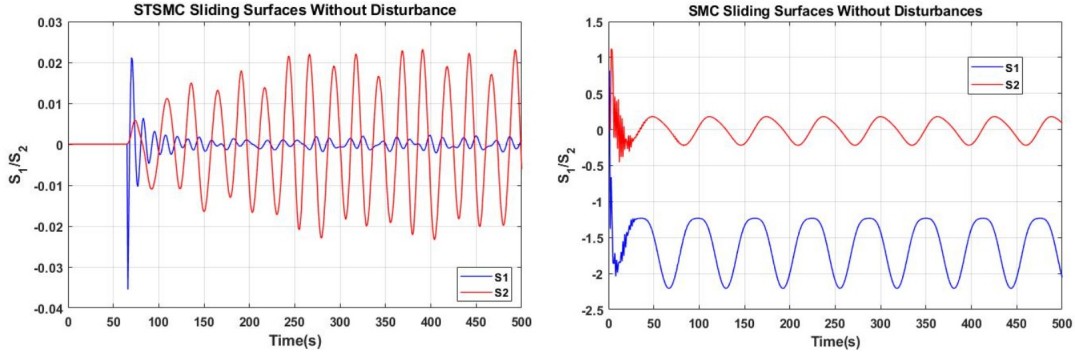Figure 4.5: Total Control Input Without Disturbance

Figure 4.6: Sliding Surfaces (Without Disturbance)

4.2 Adding Matched Disturbance Scenario

In this section, the ground vehicle performance is tested under matched disturbance ($d_V = 3m/s, d_W = 0.7rad/s$) that is added to the vehicle model. Note that this injected disturbance is considered relatively large as it exceeds half of the constraints' boundaries. Fig. 4.7 shows the trajectory tracking performance of the proposed control law for both cases (TMPC+SMC) and (TMPC+STSMC) versus the nominal MPC alone,SMC,and Lyapunov based controller . As observed, despite the addition of an input disturbance at $t = 65$, both proposed controllers (TMPC+SMC/STSMC) and SMC compensate for the injected disturbance and promptly reject it, whereas both the nominal MPC and the Lyapunov based controller are not able to reject the effect of the perturbed input, which leads to

29

unacceptable tracking performance.
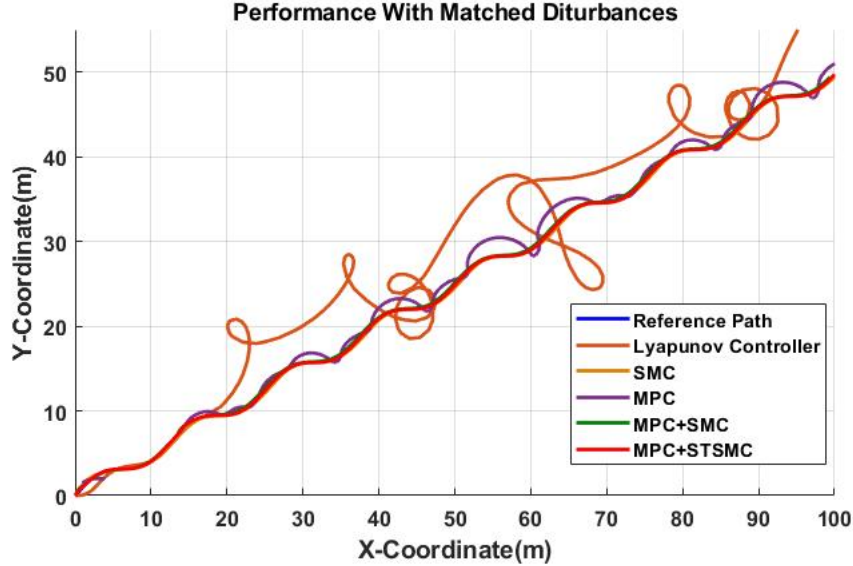

Performance With Matched Diturbances

Figure 4.7: Trajectories with an added matched disturbance. SMC, (MPC+SMC) and (MPC+STSMC) show robustness by tracking the trajectory in the presence of a matched disturbance, whereas both the nominal MPC and Lyapunov controller should be modified to account for disturbances.

The trajectory tracking simulation results emphasize the importance of integrating MPC with SMC algorithms for AGVs, since the vehicle tracks a relatively complex predefined trajectory with minimum error, as seen in Fig. 4.8, which is due to the limited prediction capability of MPC over a finite horizon, and the additive disturbance rejection ability of SMC algorithms.

Fig. 4.9 and Fig. 4.10 show the linear and angular velocities for both cases of the proposed controller, TMPC aided by STSMC and SMC, respectively. The results demonstrate the critical complementary role that the auxiliary SMC controller plays in aiding the nominal MPC when the matched disturbance occurs. when a disturbance is injected, the nominal MPC alone is not capable of attaining acceptable tracking performance as was shown in Fig. 4.7, which necessitates the intervention of the SMC to account for the induced disturbance, as shown in Fig. 4.9 and Fig. 4.10. Furthermore, Fig. 4.9 illustrates the ability of STSMC in aiding the MPC by rejecting the matched disturbances via a smooth control sig-
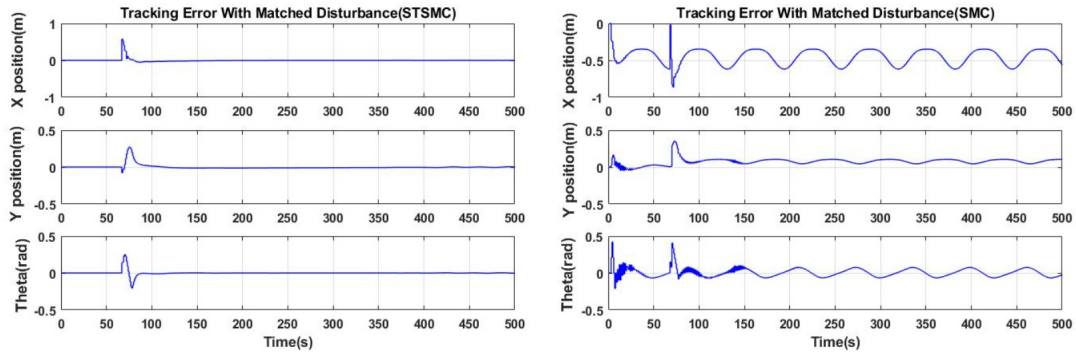
Figure 4.8: Tracking Error With Matched Disturbance

nal. On the contrary, SMC rejects the matched disturbance with a noisy control signal, as shown in Fig. 4.10.
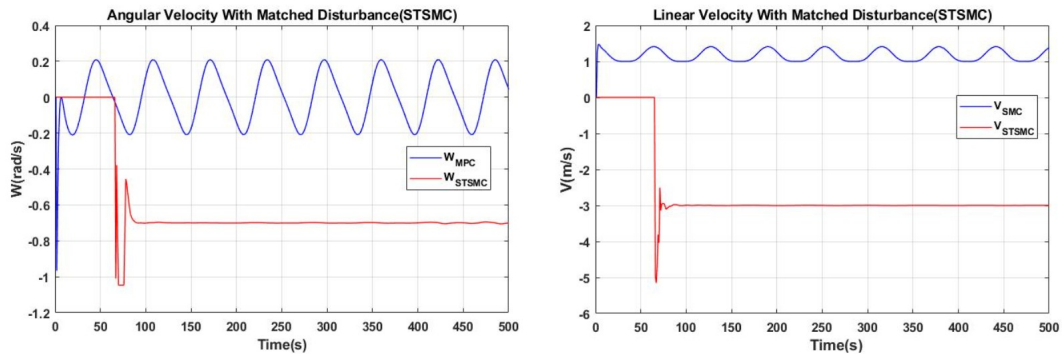

Figure 4.9: Control Inputs With Matched Disturbance (STSMC)

The original input constraints are satisfied for the (TMPC+STSMC) system, where the control actions remain within the thresholds of the original constraints (red and yellow lines), as shown in Fig. 4.11. This demonstrates the effect of tightening the constraints in Section 3.3.1. However,the (TMPC+SMC) system is not able to satisfy the original constraints due to the noisy signal generated by the SMC. Finally, Fig. 4.12 shows that the sliding surfaces of the STSMC algorithm converge to zero, whereas those of the SMC do not. The variation in SMC sliding surfaces observed in Fig. 4.12 is caused by disturbances and uncertainties.
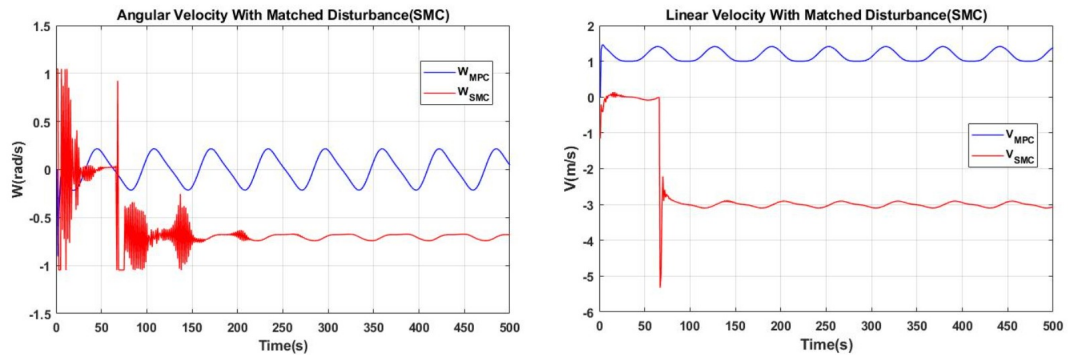
31

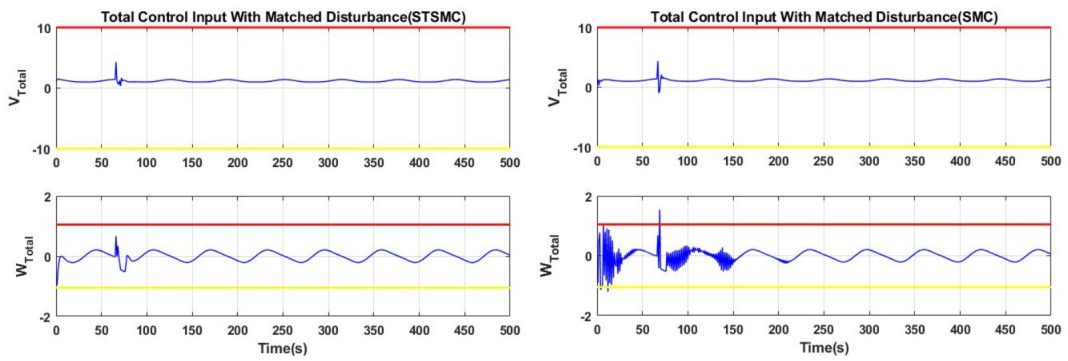Figure 4.10: Control Inputs With Matched Disturbance (SMC)

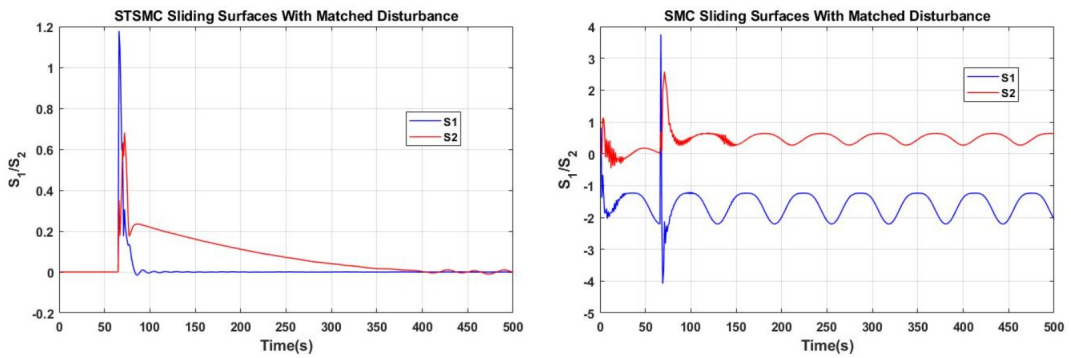Figure 4.11: Total Control Input With Matched Disturbance

Figure 4.12: Sliding Surfaces (With Matched Disturbance)

4.3 Adding Matched and Unmatched Disturbances Scenario

In this section, the simulation results demonstrate the capability of the proposed control system (TMPC+STSMC) in accomplishing the control objectives in the presence of matched ($d_V = 3m/s, d_W = 0.7rad/s$) and unmatched ($\omega_x/\omega_y = 0.6m$) disturbances. Fig. 4.13 presents the trajectory tracking performance of the (TMPC+STSMC) scheme. As observed, despite the addition of matched and unmatched disturbances, the proposed controller compensates for the injected disturbances and promptly rejects them. Also note that the integration terms, which are added to the sliding surfaces (3.21) and (3.22) in the design of the STSMC system, minimize the steady-state error and produce an acceptable performance against matched and unmatched disturbances. Contrarily, in Fig. 4.14 the (TMPC+SMC) control scheme shows unacceptable performance in the presence of both matched and unmatched disturbances, as it fails to reduce the steady-state error caused by the disturbances addition.
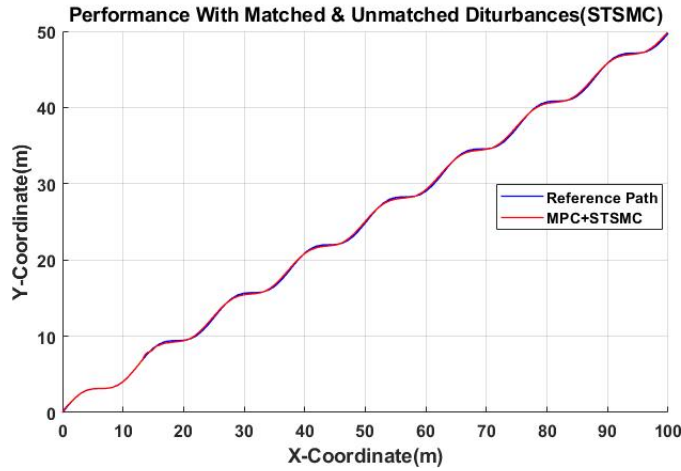

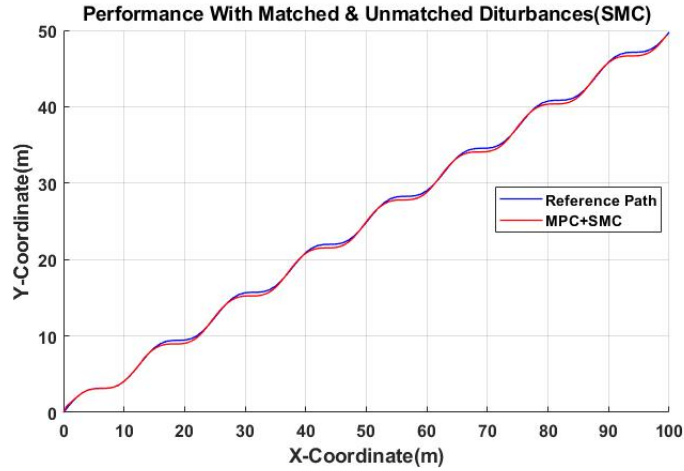Figure 4.13: Trajectories with Matched and Unmatched Disturbance (STSMC)

Figure 4.14: Trajectories with Matched and Unmatched Disturbance
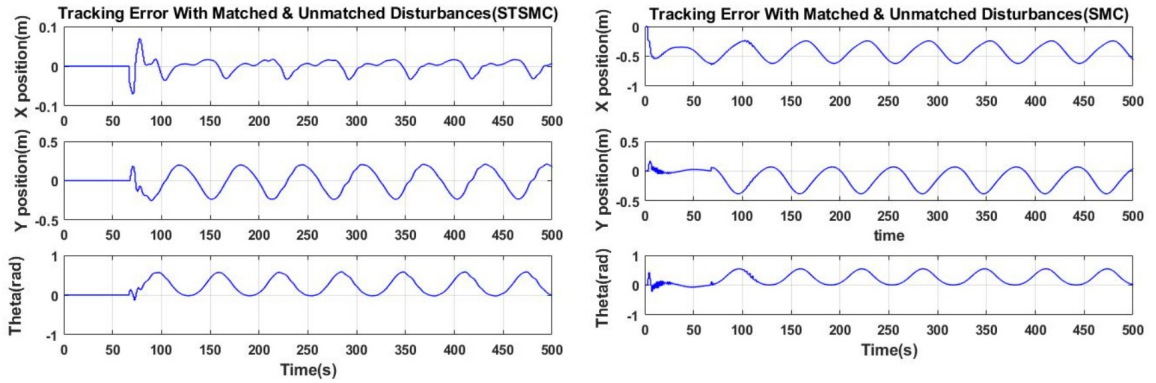
Figure 4.15: Tracking Error With Matched an Unmatched Disturbances

Despite the addition of both types of disturbances, the STSMC algorithm still provides a continuous smooth signal as present in Fig. 4.16. On the other hand, chattering severely impacts the SMC control signal, as illustrated in Fig. 4.17. The simulation results also validate the ability of the (TMPC+STSMC) algorithm in fulfilling the system constraints in this scenario, as observed in Fig. 4.18. On the other hand, Fig. 4.18 demonstrates the constraint violation caused by the noisy control signal. The sliding surfaces of STSMC in this scenario maintain convergence near zero, whereas the SMC sliding surfaces have a steady-state error, as shown in Fig. 4.19 due to the chattering phenomena.

34

Figure 4.16: Control Inputs With Matched and Unmatched Disturbance (STSMC)
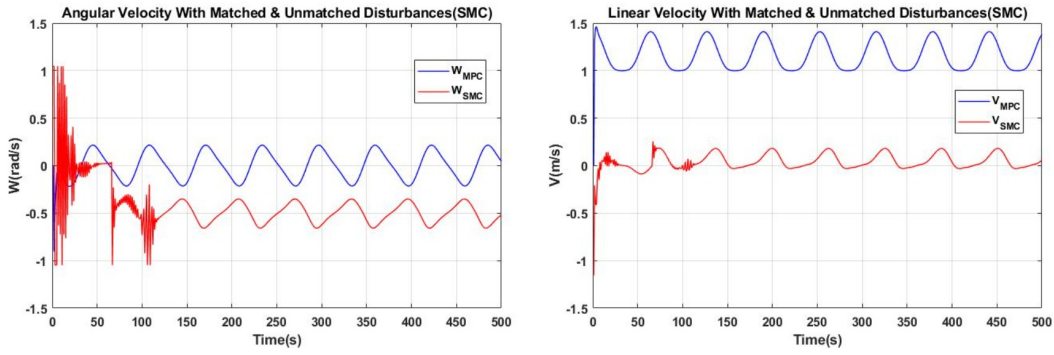
Figure 4.17: Control Inputs With Matched and Unmatched Disturbances (SMC)
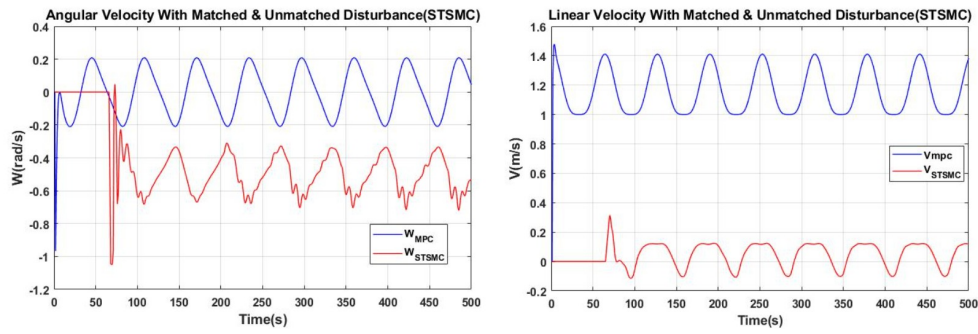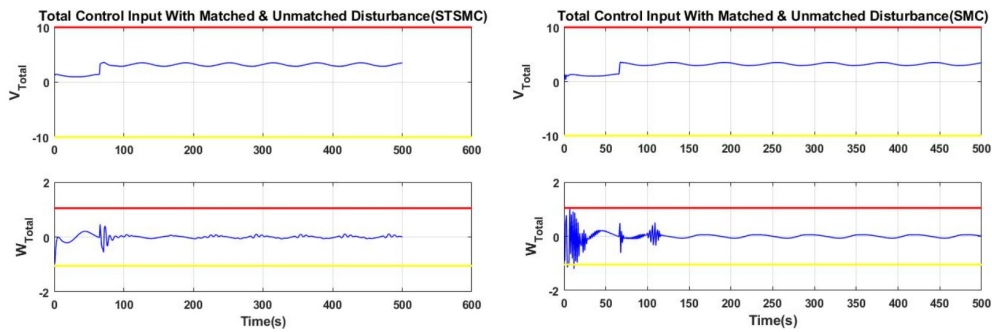

Figure 4.18: Total Control Input With Matched and Unmatched Disturbances

35
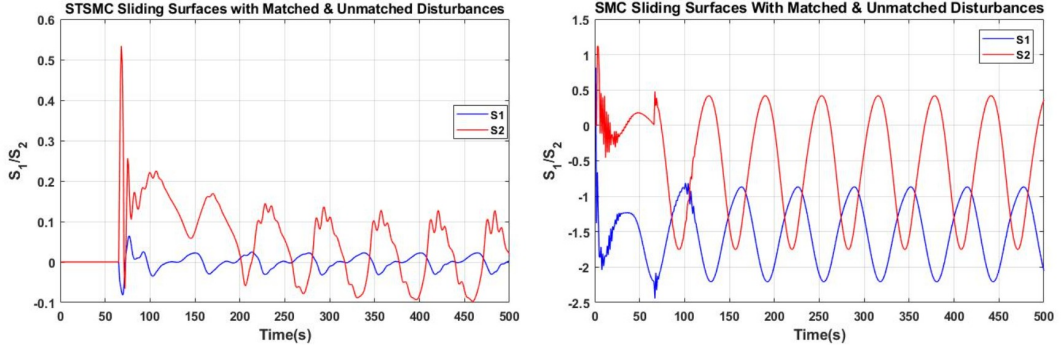
Figure 4.19: Sliding Surfaces (With Matched and Unmatched Disturbances)

4.4 Testing Different Trajectories: Circular and Eight Paths

In this section, the proposed (TMPC+STSMC) system is tested on different trajectories that are commonly used in the literature as standard trajectories (Circular and Eight Paths). The paths are defined as follows:
Circular Path:

$$
\begin{cases}
x(t) = 10 \sin 0.1t, \\
y(t) = 10 \cos 0.1t.
\end{cases}
\tag{4.2}
$$

Eight Path:

$$
\begin{cases}
x(t) = 20 \sin 0.2t, \\
y(t) = 20 \sin 0.1t.
\end{cases}
\tag{4.3}
$$

Fig. 4.20 and Fig. 4.22show the capability of the proposed (TMPC+STSMC) system to successfully track the specified trajectories. Whereas both the nominal MPC and TMPC+SMC controller show unacceptable performance in tracking the defined standard paths. As before, the control scheme guarantees obtaining minimum tracking error as well as satisfying the constraints as shown in Fig. 4.21 and Fig. 4.23.

36
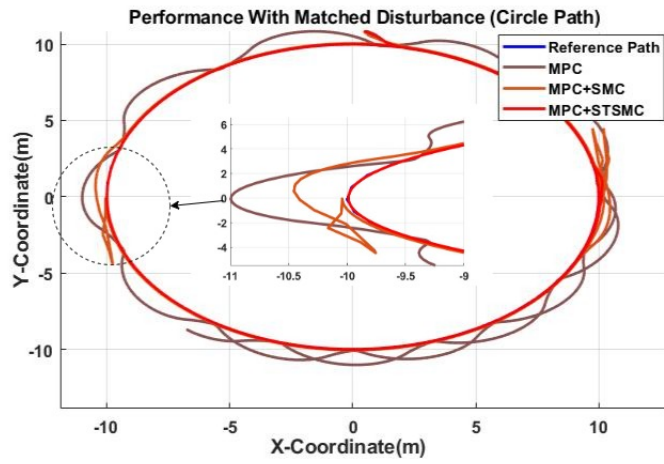
Figure 4.20: Performance With Matched Disturbance (Circle Path)
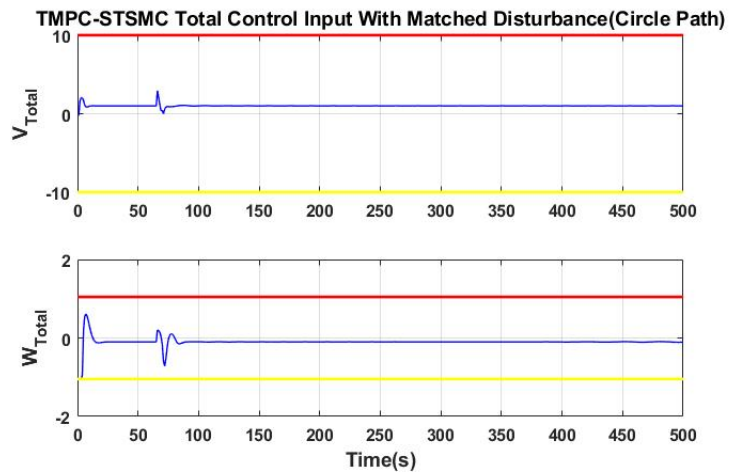
Figure 4.21: TMPC-STSMC Total Control Input With Matched Disturbance (Circle Path)
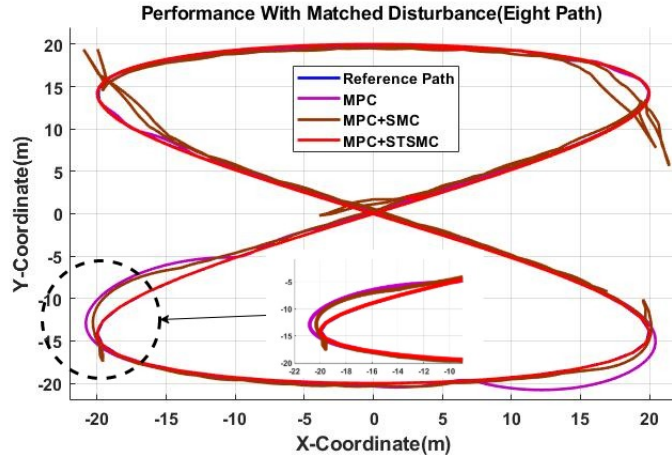
Figure 4.22: Performance With Matched Disturbance (Eight Path)
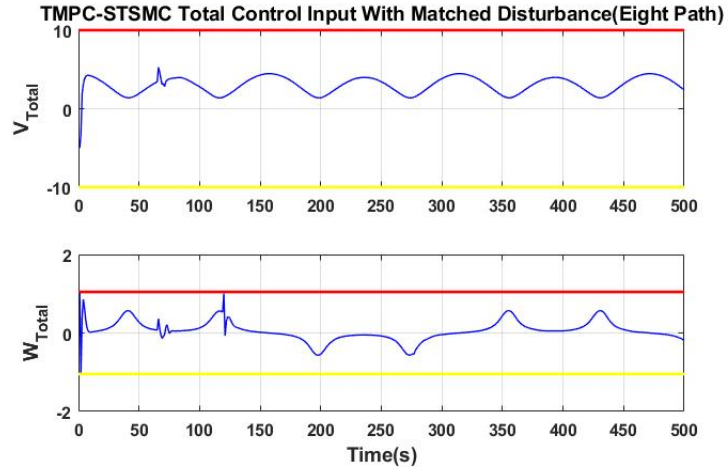
Figure 4.23: TMPC-STSMC Total Control Input With Matched Disturbance (Eight Path)

4.5 Obstacle Avoidance

This section demonstrates the ability of the proposed (TMPC+STSMC) system to avoid obstacles. In Fig. 4.24, the vehicle avoids two obstacles along its path by integrating the clearance distance constraint in (3.12) into the MPC problem formulation.
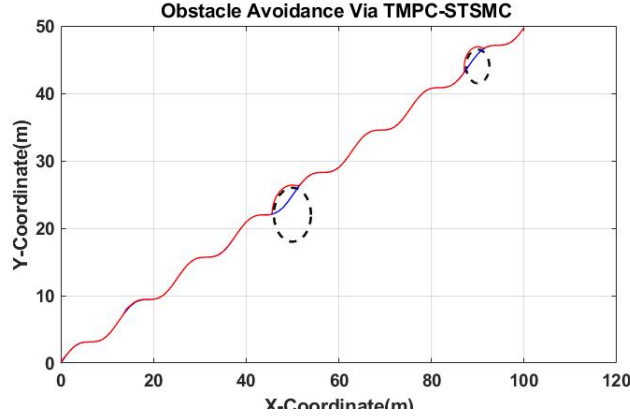
Figure 4.24: Obstacle Avoidance Via TMPC-STSMC

4.6 Comparing Controllers via Performance Indices (ISE/IAE/ITAE)

In this section, three trajectory tracking performance indices are adopted to compare the performance of the designed controllers: integral squared error (ISE), integral absolute error (IAE), and integral time-weighted absolute error (ITAE). The indices are defined as follows, where e is the tracking error between the predefined trajectory and the actual states of the AVG:

$$ISE = \int_0^T e^2(t)\,dt, \tag{4.4}$$

$$IAE = \int_0^T |e(t)|\,dt, \tag{4.5}$$

$$ITAE = \int_0^T t|e(t)|\,dt. \tag{4.6}$$

Table 4.1 shows the ISE, IAE, and ITAE values of the simulation results of the tracking problem of a ground vehicle following a sinusoidal trajectory using MPC alone, (MPC+SMC), and (TMPC+STSMC). The comparison shows clearly that the MPC+STSMC algorithm gives acceptable performances and it's more robust than MPC and MPC+STSMC algorithms.

39

		ISE	IAE	ITAE(*1.0e+04)
Lyapunov	e_x	510	153	0.4
	e_y	25	29	0.0073
SMC	e_x	131	111	2.6
	e_y	2.5	11	0.2
MPC	e_x	1.6	404	10
	e_y	0.07	77	2
MPC+SMC	e_x	21	45	2
	e_y	0.06	2	0.04
MPC+STSMC	e_x	0.001	0.2	0.000042
	e_y	0.0006	0.2	0.000059

Table 4.1: Quantitative comparison between the proposed MPC+STSMC, MPC+SMC, MPC ,SMC, and Lyapunov controllers for the sinusoidal maneuver in (4.1).

4.7 Validation in ROS Environment

4.7.1 Simulation in ROS Environment

This section provides an overview of the different autonomy subsystems that were implemented in Robot operating system (ROS) on an autonomous ground vehicle research platform, NV-X1 Electric Vehicle shown in Fig. 4.25, which is available at the American University of Beirut (AUB). The proposed trajectory tracking control system is simulated and validated in the ROS environment. ROS was introduced in [82] to serve as tool that boosts researchers' productivity while solving wide-spanning robotics problems. It is a flexible structure for developing robot software, and it contains a collection of tools and libraries that simplify simulation and implementation across a broad range of robotic platforms.

The flowchart in Fig. 4.26 demonstrates the communication within the two autonomy subsystems: perception and planning. A 3D-Lidar is used for more reliable localization and mapping by means of generating a 3D point cloud that produces an offline map. The 3D point cloud is used to provide the planning and control subsystems with accurate vehicle localization for improved navigation. ROS packages that were developed by AUTOWARE Foundation [83] were used

Figure 4.25: NV-X1 Electric Vehicle

given that they are open-source codes specifically designed for self-driving vehicles applications.

The path planner is based on the A* algorithm, which uses an occupancy grid to search for optimal solutions from the initial point to the goal. While optimality is guaranteed with A*, its main drawback lies in its large computational burden.

The proposed controller (TMPC+STSMC) completes the autonomy system by generating commands to the low-level actuator controllers. This enables the vehicle to track the planned trajectory in presence of uncertainties and disturbances. An Arduino UNO microcontroller is used to transform the control signals generated by the controller into executable commands addressed to vehicle actuators (throttle/braking/steering).

Numerical simulations using the simulation loop in Fig. 4.27 were executed to validate the proposed controller within the ROS environment. As shown in Fig. 4.28, the vehicle is able to track the planned trajectory. RVIZ - visualization tool in ROS - is used to plot the path generated by the A* algorithm (black line) and the actual vehicle trajectory (green line).
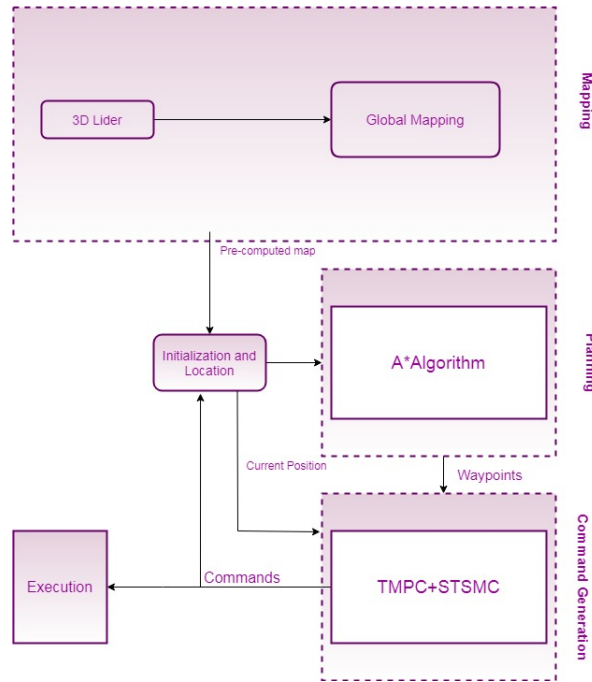
Figure 4.26: Flowchart Summarizing the autonomy subsystems of the NV-X1 Electric Vehicle platform, starting from sensing and mapping and ending with planned path execution.
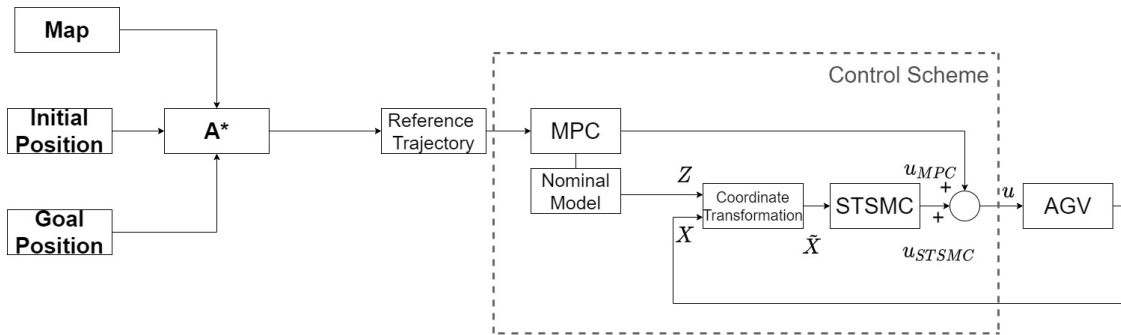
Figure 4.27: Simulation Loop Applied in ROS

4.7.2 Experimental Validation in ROS Environment(Pure Pursuit)

In addition to the numerical simulations, experimental testing was also conducted to validate the autonomy subsystems integrated into ROS. Fig. 4.29 shows the
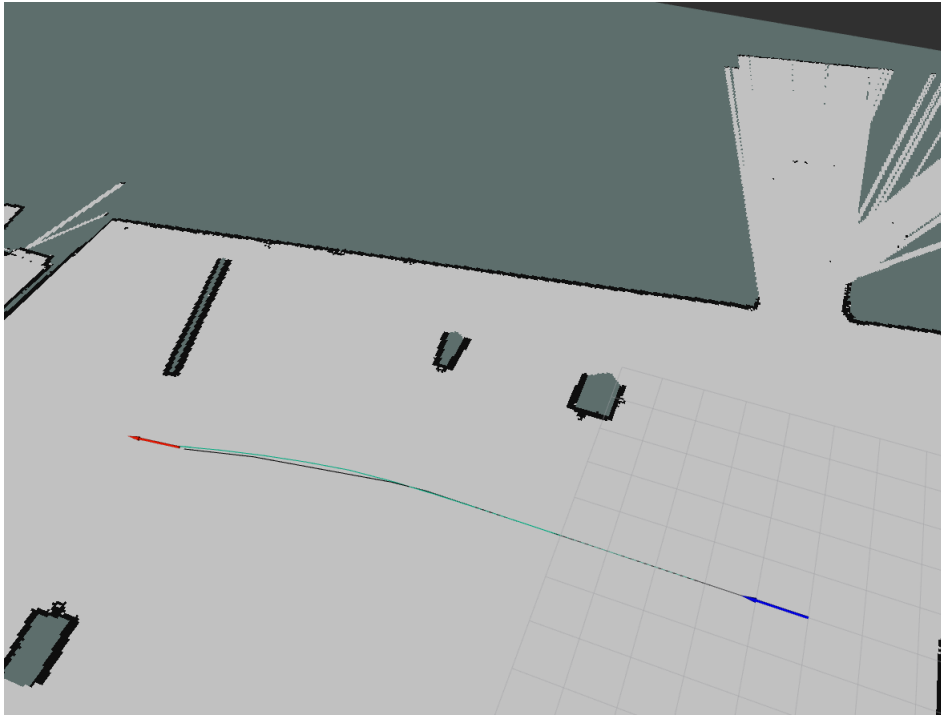
Figure 4.28: Tracking Performance in ROS Environment. The Map is for the IOEC B2 Parking Structure at AUB.

path generated by the A* algorithm while taking into consideration the offline map. However, it is noted that in this experimental validation, the pure pursuit algorithm was used to have the vehicle track the generated path by providing the high-level control commands (linear and angular velocities) to Arduino via serial communication. Moreover, the 3D Lidar runs online to provide the current vehicle position as feedback for the controller to close the loop. The communication and integration of the autonomy subsystems in the ROS environment are presented in Fig. 4.30.

43
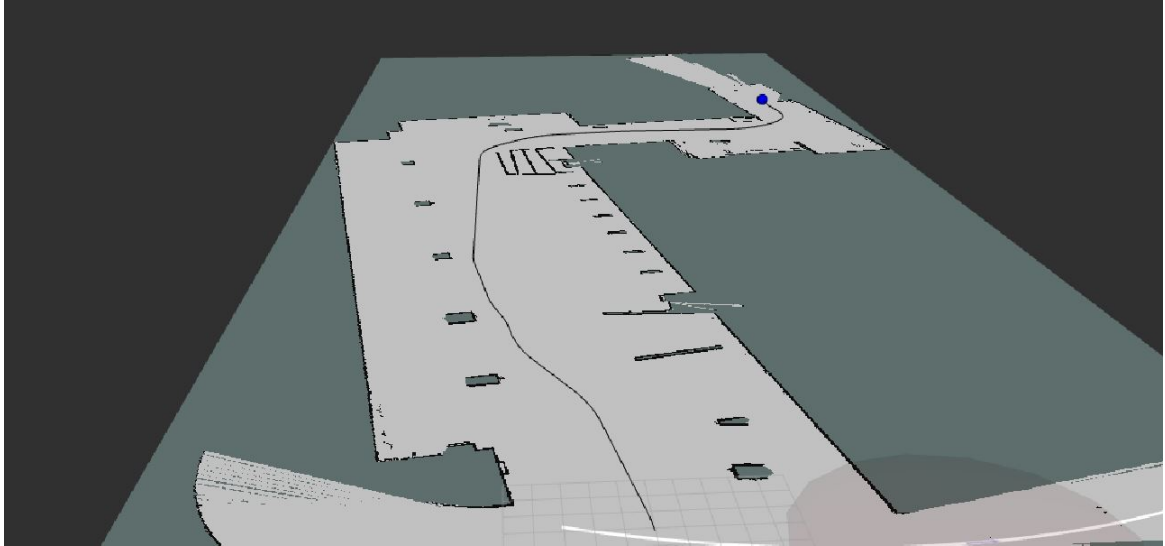
Figure 4.29: Tracked Path in the Experimental Testing. The Map is for the IOEC B2 Parking Structure at AUB (via Pure Pursuit)
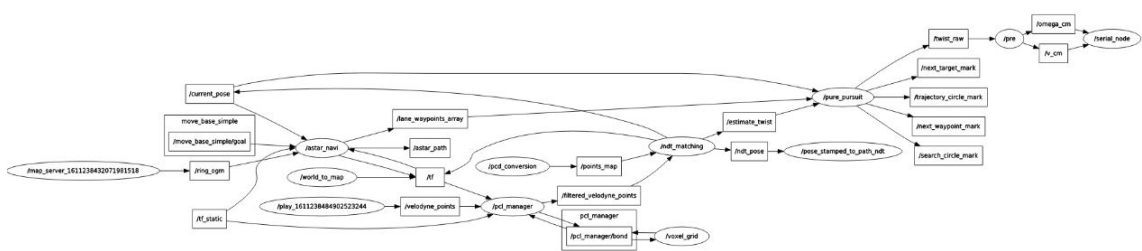
Figure 4.30: Autonomy System ROS Packages and Nodes communication in ROS (via Pure Pursuit)

Chapter 5

Conclusion and Future Work

This thesis presents the design strategy of a robust and optimal control scheme to enhance the trajectory tracking performance of autonomous ground vehicles. The proposed control system entails the combination of a nominal model predictive controller and an auxiliary sliding mode controller, which falls under the umbrella of tube-based MPC, but is developed for the nonlinear kinematic model of AGVs for the first time in this work. First-order SMC (FOSMC) and super twisting SMC (STSMC) are designed as auxiliary controllers. The super twisting sliding mode algorithm has the advantage of overcoming chattering in the control signal, which is the main drawback of the FOSMC system.

The nominal MPC component generates an optimal control effort to track a desired trajectory while fulfilling the involved constraints, and the SMC algorithm aids it by rejecting disturbances and compensating for uncertainties that induce deviations from the nominal model. The proposed control system's stability is proven by leveraging Input-to-State Stability (ISS) and Lyapunov stability theory. Simulation results demonstrate the effectiveness of the proposed control structure, and reveal a well-behaved interaction between the two sub-controllers to reach the common objective of good trajectory tracking and avoiding the obstacles, despite the presence of disturbances.

Future work includes enhancing the (MPC+STSMC) system performance in the presence of unmatched disturbances by integrating state observers in the control scheme, or designing the sliding surfaces using adaptive control theory. Last but not least, the proposed composite scheme is to be validated on an experimental AGV platform.

Appendix A

Abbreviations

MPC	Model Predictive Control
SMC	Sliding Mode Control
TMPC	Tube Based Model Predictive Control
STSMC	Super Twisting Sliding Mode Control
NMPC	Non Linear Model Predective Control.
FOSMC	First Order Sliding Mode Control
SOSMC	Second Order Sliding Mode Control
HOSMC	High Order Sliding Mode Control
ISM	Integral Sliding Mode Control
AGV	Autonomous Ground Vehicle
ISS	Input State Stability
NMR	Nonholonomic Mobile Robot
WMR	Wheeled Mobile Robot
LIDAR	Light Detection and Ranging
GPS/INS	Global Positioning System aided Inertial Navigation Systems
DARPA	Defense Advanced Research Projects Agency
PI	Proportional–Integral Controller
RHS	Receding Horizon Control
LQR	Linear–Quadratic Regulator
UAV	Unmanned Aerial Vehicle
LTI	Linear Time Invariant
ISE	Integral Squared Error,
IAE	Integral Absolute Error
ITAE	Integral Time-weighted Absolute Error.

ROS	Robot Operating System .
AUB	American University of Beirut.

Bibliography

[1] M. M. C.Jones, F. Borrelli, "Model predictive control part i – introduction," 2014.

[2] B. Paden, M. Čáp, S. Z. Yong, D. Yershov, and E. Frazzoli, "A survey of motion planning and control techniques for self-driving urban vehicles," *IEEE Transactions on intelligent vehicles*, vol. 1, no. 1, pp. 33–55, 2016.

[3] E. Thilén, "Robust model predictive control for autonomous driving," 2017.

[4] S. O.-R. A. V. S. Committee *et al.*, "Taxonomy and definitions for terms related to on-road motor vehicle automated driving systems," *SAE Standard J*, vol. 3016, pp. 1–16, 2014.

[5] K. Bimbraw, "Autonomous cars: Past, present and future a review of the developments in the last century, the present scenario and the expected future of autonomous vehicle technology," in *2015 12th International Conference on Informatics in Control, Automation and Robotics (ICINCO)*, vol. 1, pp. 191–198, IEEE, 2015.

[6] B. McKenzie and M. Rapino, "Commuting in the united states: 2009, american community survey reports, acs-15. us census bureau: Washington, dc," 2011.

[7] K. Yuan, H. Shu, Y. Huang, Y. Zhang, A. Khajepour, and L. Zhang, "Mixed local motion planning and tracking control framework for autonomous vehicles based on model predictive control," *IET Intelligent Transport Systems*, vol. 13, no. 6, pp. 950–959, 2018.

[8] L. Jaillet, J. Cortés, and T. Siméon, "Sampling-based path planning on configuration-space costmaps," *IEEE Transactions on Robotics*, vol. 26, no. 4, pp. 635–646, 2010.

[9] J. D. Rupp and A. G. King, "Autonomous driving-a practical roadmap," tech. rep., SAE Technical Paper, 2010.

[10] Y. Chen, Z. Li, H. Kong, and F. Ke, "Model predictive tracking control of nonholonomic mobile robots with coupled input constraints and unknown dynamics," *IEEE Transactions on Industrial Informatics*, vol. 15, no. 6, pp. 3196–3205, 2018.

[11] J. López, C. Otero, R. Sanz, E. Paz, E. Molinos, and R. Barea, "A new approach to local navigation for autonomous driving vehicles based on the curvature velocity method," in *2019 International Conference on Robotics and Automation (ICRA)*, pp. 1751–1757, 2019.

[12] Y. Dai, D. Jia, L. Guo, S. Ye, D. Luo, W. Hu, and W. Peng, "Backstepping controller for trajectory tracking of wheeled mobile robot based on particle swarm optimization," in *2019 Chinese Control Conference (CCC)*, pp. 4259–4264, IEEE, 2019.

[13] M. Korayem, M. Yousefzadeh, and S. Manteghi, "Dynamics and input–output feedback linearization control of a wheeled mobile cable-driven parallel robot," *Multibody System Dynamics*, vol. 40, no. 1, pp. 55–73, 2017.

[14] J.-y. Zhai and Z.-b. Song, "Adaptive sliding mode trajectory tracking control for wheeled mobile robots," *International Journal of Control*, vol. 92, no. 10, pp. 2255–2262, 2019.

[15] T. Nascimento, C. Dorea, and L. Gonçalves, "Nonholonomic mobile robots' trajectory tracking model predictive control: a survey," *Robotica*, vol. 36, pp. 1–21, 01 2018.

[16] K. Worthmann, M. W. Mehrez, M. Zanon, G. K. Mann, R. G. Gosine, and M. Diehl, "Model predictive control of nonholonomic mobile robots without stabilizing constraints and costs," *IEEE transactions on control systems technology*, vol. 24, no. 4, pp. 1394–1406, 2015.

[17] A. Rupp and M. Stolz, *Survey on Control Schemes for Automated Driving on Highways*, pp. 43–69. Germany: Springer Verlag, 2017.

[18] J.-M. Yang and J.-H. Kim, "Sliding mode control for trajectory tracking of nonholonomic wheeled mobile robots," *IEEE Transactions on robotics and automation*, vol. 15, no. 3, pp. 578–587, 1999.

[19] P. J. Campo and M. Morari, "Robust model predictive control," in *1987 American control conference*, pp. 1021–1026, IEEE, 1987.

[20] E. Kayacan and J. Peschel, "Robust model predictive control of systems by modeling mismatched uncertainty," *IFAC-PapersOnLine*, vol. 49, no. 18, pp. 265 – 269, 2016. 10th IFAC Symposium on Nonlinear Control Systems NOLCOS 2016.

[21] R. González, M. Fiacchini, J. L. Guzmán, T. Álamo, and F. Rodríguez, "Robust tube-based predictive control for mobile robots in off-road conditions," *Robotics and Autonomous Systems*, vol. 59, pp. 711 – 726, oct 2011.

[22] M. Farrokhsiar and H. Najjaran, "A robust probing motion planning scheme: A tube-based mpc approach," in *2013 American Control Conference*, pp. 6492–6498, June 2013.

[23] M. Bahadorian, B. Savkovic, R. Eaton, and T. Hesketh, "Robust model predictive control for automated trajectory tracking of an unmanned ground vehicle," in *2012 American Control Conference (ACC)*, pp. 4251–4256, IEEE, 2012.

[24] B. T. Lopez, J. P. Howl, and J.-J. E. Slotine, "Dynamic tube mpc for nonlinear systems," in *2019 American Control Conference (ACC)*, pp. 1655–1662, IEEE, 2019.

[25] Y. Shan, W. Yang, C. Chen, J. Zhou, L. Zheng, and B. Li, "Cf-pursuit: A pursuit method with a clothoid fitting and a fuzzy controller for autonomous vehicles," *International Journal of Advanced Robotic Systems*, vol. 12, p. 134, jan 2015.

[26] M. Samuel, M. Hussein, and M. Binti, "A review of some pure-pursuit based path tracking techniques for control of autonomous vehicle," *International Journal of Computer Applications*, vol. 135, pp. 35–38, 02 2016.

[27] M. Park, S. Lee, and W. Han, "Development of lateral control system for autonomous vehicle based on adaptive pure pursuit algorithm," in *2014 14th International Conference on Control, Automation and Systems (IC-CAS 2014)*, pp. 1443–1447, Oct 2014.

[28] A. Ollero and G. Heredia, "Stability analysis of mobile robot path tracking," in *Proceedings 1995 IEEE/RSJ International Conference on Intelligent Robots and Systems. Human Robot Interaction and Cooperative Robots*, vol. 3, pp. 461–466 vol.3, Aug 1995.

[29] S. Thrun, M. Montemerlo, H. Dahlkamp, D. Stavens, A. Aron, J. Diebel, P. Fong, J. Gale, M. Halpenny, G. Hoffmann, *et al.*, "Stanley: The robot that won the darpa grand challenge," *Journal of field Robotics*, vol. 23, no. 9, pp. 661–692, 2006.

[30] J. M. Snider, "Automatic steering methods for autonomous automobile path tracking," 2009.

[31] L. Montoya-Villegas, J. Moreno-Valenzuela, and R. Pérez-Alcocer, "A feedback linearization-based motion controller for a uwmr with experimental evaluations," *Robotica*, vol. 37, no. 6, p. 1073–1089, 2019.

[32] M. H. Korayem, R. A. Esfeden, and S. R. Nekoo, "Path planning algorithm in wheeled mobile manipulators based on motion of arms," *Journal of Mechanical Science and Technology*, vol. 29, pp. 1753–1763, Apr 2015.

[33] M. Korayem, M. Yousefzadeh, and s. Manteghi, "Dynamics and input–output feedback linearization control of a wheeled mobile cable-driven parallel robot," *Multibody System Dynamics*, vol. 40, pp. 55–73, 09 2016.

[34] R. Liu, X. Sun, and D. Wang, "Heavyweight airdrop flight control design using feedback linearization and adaptive sliding mode," *Transactions of the Institute of Measurement and Control*, vol. 38, pp. 1155–1164, 02 2016.

[35] Y. Dai, D. Jia, L. Guo, S. Ye, D. Luo, W. Hu, and W. Peng, "Backstepping controller for trajectory tracking of wheeled mobile robot based on particle swarm optimization," in *2019 Chinese Control Conference (CCC)*, pp. 4259–4264, July 2019.

[36] Z.-P. JIANGdagger and H. Nijmeijer, "Tracking control of mobile robots: A case study in backstepping," *Automatica*, vol. 33, no. 7, pp. 1393–1399, 1997.

[37] Z.-P. Jiang, E. Lefeber, and H. Nijmeijer, "Saturated stabilization and tracking of a nonholonomic mobile robot," *Systems & Control Letters*, vol. 42, no. 5, pp. 327–332, 2001.

[38] I. Zohar, A. Ailon, and R. Rabinovici, "Mobile robot characterized by dynamic and kinematic equations and actuator dynamics: Trajectory tracking and related application," *Robotics and autonomous systems*, vol. 59, no. 6, pp. 343–353, 2011.

[39] S. Rudra, R. K. Barai, and M. Maitra, "Design and implementation of a block-backstepping based tracking control for nonholonomic wheeled mobile robot," *International Journal of Robust and Nonlinear Control*, vol. 26, no. 14, pp. 3018–3035, 2016.

[40] A. Bayoumi, "Wheeled mobile robot trajectory tracking using sliding mode control," *Journal of Computer Science*, vol. 12, pp. 48–55, 01 2016.

[41] R. Solea, "Sliding mode control applied in trajectory-tracking of wmrs and autonomous vehicles," 2009.

[42] J. Zhai and Z.-b. Song, "Adaptive sliding mode trajectory tracking control for wheeled mobile robots," *International Journal of Control*, vol. 92, pp. 1–16, 02 2018.

[43] Y. Guo, L. Yu, and J. Xu, "Robust finite-time trajectory tracking control of wheeled mobile robots with parametric uncertainties and disturbances," *Journal of Systems Science and Complexity*, vol. 32, pp. 1358–1374, Oct 2019.

[44] G. Wang, C. Zhou, Y. Yu, and X. Liu, "Adaptive sliding mode trajectory tracking control for wmr considering skidding and slipping via extended state observer," *Energies*, vol. 12, p. 3305, 08 2019.

[45] F. Mohd Zaihidee, S. Mekhilef, and M. Mubin, "Robust speed control of pmsm using sliding mode control (smc)—a review," *Energies*, vol. 12, no. 9, p. 1669, 2019.

[46] Y. Shtessel, C. Edwards, L. Fridman, and A. Levant, *Sliding mode control and observation*. Springer, 2014.

[47] A. Levant, "Sliding order and sliding accuracy in sliding mode control," *International journal of control*, vol. 58, no. 6, pp. 1247–1263, 1993.

[48] S. Yu, Y. Guo, L. Meng, T. Qu, and H. Chen, "Mpc for path following problems of wheeled mobile robots∗∗the work is supported by the national natural science foundation of china for financial support within the projects no. 61573165, no. 6171101085 and no. 61520106008.," *IFAC-PapersOnLine*, vol. 51, no. 20, pp. 247 – 252, 2018. 6th IFAC Conference on Nonlinear Model Predictive Control NMPC 2018.

[49] C. E. García, D. M. Prett, and M. Morari, "Model predictive control: Theory and practice—a survey," *Automatica*, vol. 25, pp. 335 – 348, may 1989.

[50] D. Simon and J. Löfberg, "Stability analysis of model predictive controllers using mixed integer linear programming," in *2016 IEEE 55th Conference on Decision and Control (CDC)*, pp. 7270–7275, Dec 2016.

[51] J. Liu, P. Jayakumar, J. L. Stein, and T. Ersal, "A nonlinear model predictive control formulation for obstacle avoidance in high-speed autonomous ground vehicles in unstructured environments," *Vehicle System Dynamics*, vol. 56, pp. 853–882, nov 2018.

[52] T. Faulwasser, *Optimization-based solutions to constrained trajectory-tracking and path-following problems*. Shaker Verlag, 01 2013.

[53] S. Yu, X. Li, H. Chen, and F. Allgöwer, "Nonlinear model predictive control for path following problems," *IFAC Proceedings Volumes*, vol. 45, no. 17, pp. 145 – 150, 2012. 4th IFAC Conference on Nonlinear Model Predictive Control.

[54] Z. Sun, L. Dai, K. Liu, Y. Xia, and K. H. Johansson, "Robust mpc for tracking constrained unicycle robots with additive disturbances," *Automatica*, vol. 90, pp. 172 – 184, apr 2018.

[55] T. Nascimento, C. Dorea, and L. Gonçalves, "Nonlinear model predictive control for trajectory tracking of nonholonomic mobile robots: A modified approach," *International Journal of Advanced Robotic Systems*, vol. 15, p. 172988141876046, 02 2018.

53

[56] Z. Sun, L. Dai, Y. Xia, and K. Liu, "Event-based model predictive tracking control of nonholonomic systems with coupled input constraint and bounded disturbances," *IEEE Transactions on Automatic Control*, vol. 63, pp. 608–615, Feb 2018.

[57] A. Bemporad and M. Morari, "Robust model predictive control: A survey," in *Robustness in identification and control*, pp. 207–226, Springer, 1999.

[58] S. Dixit, S. Fallah, U. Montanaro, M. Dianati, A. Stevens, F. Mccullough, and A. Mouzakitis, "Trajectory planning and tracking for autonomous overtaking: State-of-the-art and future prospects," *Annual Reviews in Control*, vol. 45, pp. 76–86, 2018.

[59] D. L. Marruedo, T. Alamo, and E. Camacho, "Input-to-state stable mpc for constrained discrete-time nonlinear systems with bounded additive uncertainties," in *Proceedings of the 41st IEEE Conference on Decision and Control, 2002.*, vol. 4, pp. 4619–4624, IEEE, 2002.

[60] D. L. Marruedo, T. Alamo, and E. Camacho, "Stability analysis of systems with bounded additive uncertainties based on invariant sets: Stability and feasibility of mpc," in *Proceedings of the 2002 American Control Conference (IEEE Cat. No. CH37301)*, vol. 1, pp. 364–369, IEEE, 2002.

[61] M. Bahadorian, B. Savkovic, R. Eaton, and T. Hesketh, "Toward a robust model predictive controller applied to mobile vehicle trajectory tracking control," *IFAC Proceedings Volumes*, vol. 44, no. 1, pp. 13552–13557, 2011.

[62] D. Mayne, M. Seron, and S. Raković, "Robust model predictive control of constrained linear systems with bounded disturbances," *Automatica*, vol. 41, pp. 219 – 224, feb 2005.

[63] S. Rakovic, A. Teel, D. Mayne, and A. Astolfi, "Simple robust control invariant tubes for some classes of nonlinear discrete time systems," in *Proceedings of the 45th IEEE Conference on Decision and Control*, pp. 6397–6402, IEEE, 2006.

[64] P. Falugi and D. Q. Mayne, "Tube-based model predictive control for nonlinear systems with unstructured uncertainty," in *2011 50th IEEE Conference on Decision and Control and European Control Conference*, pp. 2656–2661, IEEE, 2011.

[65] P. Falugi and D. Q. Mayne, "Getting robustness against unstructured uncertainty: a tube-based mpc approach," *IEEE Transactions on Automatic Control*, vol. 59, no. 5, pp. 1290–1295, 2013.

[66] S. Yu, C. Maier, H. Chen, and F. Allgöwer, "Tube mpc scheme based on robust control invariant set with application to lipschitz nonlinear systems," *Systems & Control Letters*, vol. 62, no. 2, pp. 194–200, 2013.

[67] H. S. Abbas, G. Männel, C. H. né Hoffmann, and P. Rostalski, "Tube-based model predictive control for linear parameter-varying systems with bounded rate of parameter variation," *Automatica*, vol. 107, pp. 21–28, 2019.

[68] M. A. Santos, A. Ferramosca, and G. V. Raffo, "Tube-based mpc with nonlinear control for load transportation using a uav," *IFAC-PapersOnLine*, vol. 51, no. 25, pp. 459–465, 2018.

[69] P. Wang, X. Feng, and W. Li, "Design of robust positively invariant set for nonholonomic vehicle," in *2016 Chinese Control and Decision Conference (CCDC)*, pp. 814–819, May 2016.

[70] K. R. Muske, H. Ashrafiuon, and M. Nikkhah, "A predictive and sliding mode cascade controller," in *2007 American Control Conference*, pp. 4540–4545, 2007.

[71] M. Spasic, M. Hovd, D. Mitic, and D. Antic, "Tube model predictive control with an auxiliary sliding mode controller," 2016.

[72] M. Spasic, D. Miti, M. Hovd, and D. Antic, "Tube model predictive control based on laguerre functions with an auxiliary sliding mode controller," in *2017 IEEE 15th International Symposium on Intelligent Systems and Informatics (SISY)*, pp. 000243–000248, IEEE, 2017.

[73] M. Rubagotti, D. M. Raimondo, A. Ferrara, and L. Magni, "Robust model predictive control with integral sliding mode in continuous-time sampled-data nonlinear systems," *IEEE Transactions on Automatic Control*, vol. 56, no. 3, pp. 556–570, 2010.

[74] I. M.-B. Hassine, M. W. Naouar, and N. Mrabet-Bellaaj, "Model predictive-sliding mode control for three-phase grid-connected converters," *IEEE Transactions on Industrial Electronics*, vol. 64, no. 2, pp. 1341–1349, 2016.

[75] D. J. Kim, C. M. Kang, S.-H. Lee, and C. C. Chung, "Discrete-time integral sliding model predictive control for dynamic lateral motion of autonomous driving vehicles," in *2018 Annual American Control Conference (ACC)*, pp. 4757–4763, IEEE, 2018.

[76] R. C. Solea, *Sliding mode control applied in trajectory-tracking of WMRs and autonomous vehicles*. PhD thesis, 2009.

[77] W. Gao and J. C. Hung, "Variable structure control of nonlinear systems: A new approach," *IEEE transactions on Industrial Electronics*, vol. 40, no. 1, pp. 45–55, 1993.

[78] D. Limon, T. Alamo, D. M. Raimondo, D. M. De La Peña, J. M. Bravo, A. Ferramosca, and E. F. Camacho, "Input-to-state stability: a unifying framework for robust model predictive control," in *Nonlinear model predictive control*, pp. 1–26, Springer, 2009.

[79] J. A. Moreno and M. Osorio, "A lyapunov approach to second-order sliding mode controllers and observers," in *2008 47th IEEE conference on decision and control*, pp. 2856–2861, IEEE, 2008.

[80] J. A. E. Andersson, J. Gillis, G. Horn, J. B. Rawlings, and M. Diehl, "CasADi – A software framework for nonlinear optimization and optimal control," *Mathematical Programming Computation*, In Press, 2018.

[81] Y. Kanayama, Y. Kimura, F. Miyazaki, and T. Noguchi, "A stable tracking control method for an autonomous mobile robot," in *Proceedings., IEEE International Conference on Robotics and Automation*, pp. 384–389, IEEE, 1990.

[82] M. Quigley, K. Conley, B. Gerkey, J. Faust, T. Foote, J. Leibs, R. Wheeler, and A. Y. Ng, "Ros: an open-source robot operating system," in *ICRA workshop on open source software*, vol. 3, p. 5, Kobe, Japan, 2009.

[83] S. Kato, S. Tokunaga, Y. Maruyama, S. Maeda, M. Hirabayashi, Y. Kitsukawa, A. Monrroy, T. Ando, Y. Fujii, and T. Azumi, "Autoware on board: Enabling autonomous vehicles with embedded systems," in *2018 ACM/IEEE 9th International Conference on Cyber-Physical Systems (ICCPS)*, pp. 287–296, IEEE, 2018.